Convection in solid planetary interiors and implications for their evolution

S. Labrosse

LGL-TPE, Université Claude Bernard Lyon 1, Ens de Lyon, CNRS

FDEPS, Nov. 2019

Subsolidus convection

- Solid surface planets and planetary objects (icy satellites, dwarf planets) show signs of deformation in the solid state, whether active or in their past.
- In many cases: thermal convection.
- Very large viscosity $\Longrightarrow$ slow motion. The bottleneck for the thermal evolution of planetary objects with solid surface.
- In many cases, a liquid layer exists below (metallic core, water ocean) whose dynamics is controlled by the rate of heat extraction by convection in the solid.
- Convection can also happen in solid shells or spheres deep inside planetary objects: inner core, HP ice layers of Titan, Ganymede.

$\Longrightarrow$ Important to understand convection in planetary mantles.

Part I

Fundamentals of Rayleigh-Bénard convection

Bénard (1900a,b, 1901) conducted the first systematic experiments on flow driven by a destabilising temperature difference.

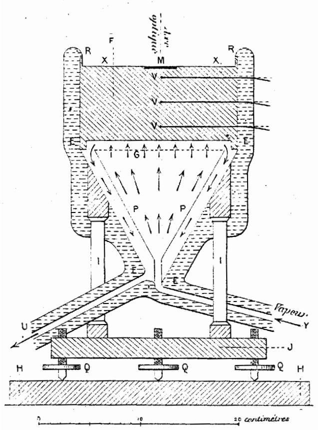

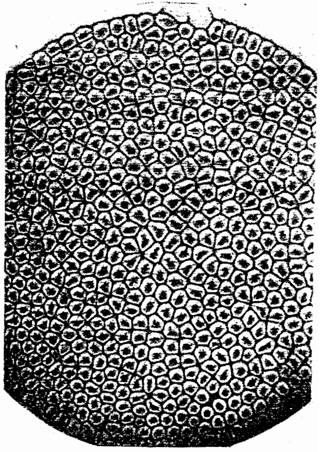

- Organisation of the flow in nearly perfect hexagonal cells (analogy to plant cells).

- Rayleigh (1916) proposed the first theory for the linear stability of a steady conductive state in a gravity field. He showed that a minimum temperature gradient is necessary for the onset of convection, that depends on several physical parameters.
- Block (1956) showed that the flow in Bénard's experiments is not driven by gravity but by temperature–dependence of surface tension, the Marangoni effect. Pearson (1958) developed the corresponding theory.
- Rayleigh–Bénard convection is still used to denote convection driven by the temperature–dependence of density in a gravity field while Bénard's setup is called Bénard–Marangoni.

(Bénard, 1901)
Topography exaggerated 100x

Fig. 15.

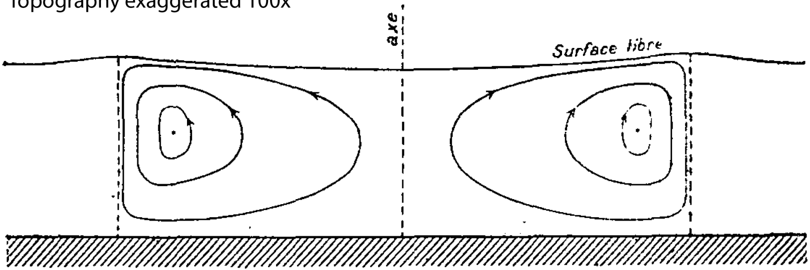

In order to pose a fluid dynamical problem, we write:

- Conservations equations: mass, momentum, energy.
  - Well established, universal although several level of approximations are possible.
- Boundary conditions (BC): classical ones (Dirichlet, Neumann, Robin) or more exotic (phase change BC).
- Constitutive equations: Fourier's law, rheology, equation of state.
  - Can be quite complex.
  - Generally poorly constrained for the planetary interiors.

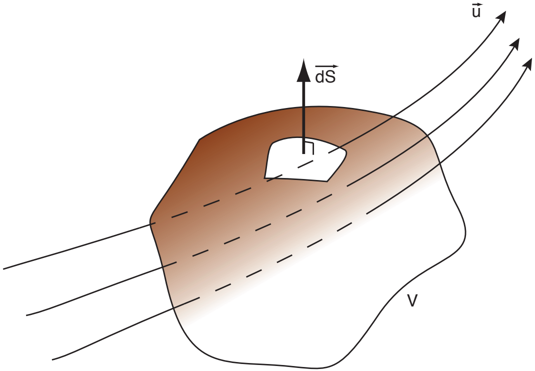

- Consider a fixed control volume.
- The balance equation for a quantity with mass density f is written:

$$\frac{\partial}{\partial t}\int_V \rho f \,\mathrm{d}V = -\int_S \boldsymbol{J_f}\cdot\mathbf{d}\boldsymbol{S} + \int_V \sigma_f \,\mathrm{d}V$$

where the flux $\boldsymbol{J_f}$ and the production σ_f express basic laws of physics.

- Use Gauss' theorem:

$$\Rightarrow \frac{\partial \rho f}{\partial t} = -\boldsymbol{\nabla}\cdot\boldsymbol{J_f} + \sigma_f$$

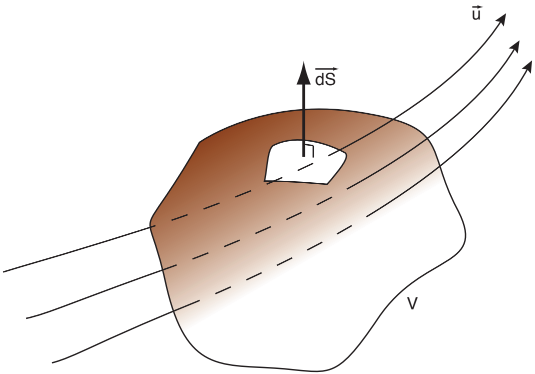

- Consider a fixed control volume.
- The balance equation for a quantity with mass density f is written:

$$\frac{\partial}{\partial t}\int_V \rho f \, \mathrm{d}V = -\int_S \boldsymbol{J_f} \cdot \mathbf{d}\boldsymbol{S} + \int_V \sigma_f \, \mathrm{d}V$$

where the flux $\boldsymbol{J_f}$ and the production σ_f express basic laws of physics.

- Use Gauss' theorem:

$$\Rightarrow \frac{\partial \rho f}{\partial t} = -\boldsymbol{\nabla} \cdot \boldsymbol{J_f} + \sigma_f$$

Conservation equations

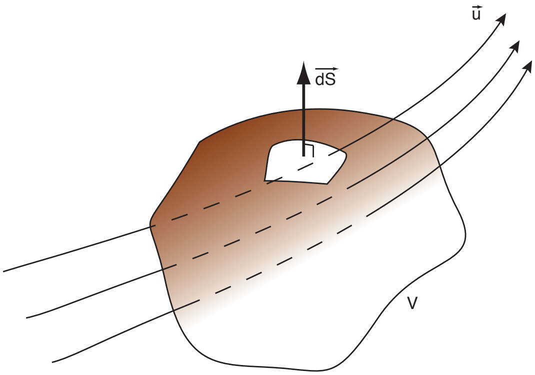

- Consider a fixed control volume.
- The balance equation for a quantity with mass density f is written:

$$\frac{\partial}{\partial t}\int_V \rho f \,\mathrm{d}V = -\int_S \boldsymbol{J_f}\cdot\mathbf{d}\boldsymbol{S} + \int_V \sigma_f \,\mathrm{d}V$$

where the flux $\boldsymbol{J_f}$ and the production σ_f express basic laws of physics.

- Use Gauss' theorem:

$$\Rightarrow \frac{\partial \rho f}{\partial t} = -\boldsymbol{\nabla}\cdot\boldsymbol{J_f} + \sigma_f$$

- No production: $\Rightarrow \sigma_f = 0$
- Convective flow only: $\boldsymbol{J_f} = \rho \boldsymbol{u}$

$$\frac{\partial}{\partial t}\int_V \rho \,\mathsf{d}\,V = -\int_S \rho \boldsymbol{u}\cdot \mathbf{d}\boldsymbol{S} \Rightarrow \int_V \frac{\partial \rho}{\partial t}\,\mathsf{d}\,V = -\int_V \boldsymbol{\nabla}\cdot(\rho \boldsymbol{u})\,\mathsf{d}\,V$$

$$\Rightarrow \frac{\partial \rho}{\partial t} + \boldsymbol{u}\cdot\boldsymbol{\nabla}\rho \equiv \frac{\mathsf{D}\rho}{\mathsf{D}t} = -\rho\boldsymbol{\nabla}\cdot\boldsymbol{u}$$

- Incompressible flow: $\boldsymbol{\nabla}\cdot\boldsymbol{u} = 0$.
- Note

$$\frac{\mathsf{D}}{\mathsf{D}t} \equiv \frac{\partial}{\partial t} + \boldsymbol{u}\cdot\boldsymbol{\nabla}.$$

Momentum

$$\rho \frac{\mathrm{D}\boldsymbol{u}}{\mathrm{D}t} = -\boldsymbol{\nabla} P + \boldsymbol{\nabla} \cdot \boldsymbol{\tau} + \rho \boldsymbol{g}$$

Local expression of Newton's 2^{nd} law with

- forces applied to the surface: pressure P and deviatoric stress $\boldsymbol{\tau}$.
- body forces: gravity $\rho \boldsymbol{g}$.
- Other terms need to be added when dealing with other planetary layers: Coriolis acceleration, Lorentz force.

Energy conservation

First principle of thermodynamics leads to:

$$\rho \frac{\mathrm{D}\,e}{\mathrm{D}t} = -\boldsymbol{\nabla} \cdot \boldsymbol{q} - P\boldsymbol{\nabla} \cdot \boldsymbol{u} + \boldsymbol{\tau} : \boldsymbol{\nabla}\boldsymbol{u} + \rho h$$

Includes

- Viscous dissipation: $\boldsymbol{\tau} : \boldsymbol{\nabla}\boldsymbol{u}$
- Radiogenic or tidal heat production: ρh

- Internal energy e is developed as function of two state variables s and ρ (add composition if necessary).

$$\mathrm{d}e = T\,\mathrm{d}S - P\,\mathrm{d}V \rightarrow \frac{\mathrm{D}e}{\mathrm{D}t} = T\,\frac{\mathrm{D}s}{\mathrm{D}t} + \frac{P}{\rho^2}\,\frac{\mathrm{D}\rho}{\mathrm{D}t}$$

- Combine the equation for internal energy:

$$\rho T\,\frac{\mathrm{D}s}{\mathrm{D}t} = -\boldsymbol{\nabla}\cdot\boldsymbol{q} + \boldsymbol{\tau} : \boldsymbol{\nabla}\boldsymbol{u} + \rho h$$

- In the generic form of a conservation equation:

$$\rho\,\frac{\mathrm{D}s}{\mathrm{D}t} = \underbrace{-\boldsymbol{\nabla}\cdot\frac{\boldsymbol{q}}{T}}_{echange} + \underbrace{\frac{-1}{T^2}\boldsymbol{q}\cdot\boldsymbol{\nabla}T + \frac{\boldsymbol{\tau} : \boldsymbol{\nabla}\boldsymbol{u} + \rho H}{T}}_{production \geq 0}$$

Equation for the temperature

Depending on the choice of state variable, (T, P) or (T, ρ):

$$\rho C_p \frac{\mathsf{D}\,T}{\mathsf{D}t} = -\boldsymbol{\nabla} \cdot \boldsymbol{q} + \alpha\, T \frac{DP}{Dt} + \boldsymbol{\tau} : \boldsymbol{\nabla} \boldsymbol{u} + \rho h$$

$$\rho C_V \frac{\mathsf{D}\,T}{\mathsf{D}t} = -\boldsymbol{\nabla} \cdot \boldsymbol{q} + \alpha\, T K_T \boldsymbol{\nabla} \cdot \boldsymbol{u} + \boldsymbol{\tau} : \boldsymbol{\nabla} \boldsymbol{u} + \rho h$$

In the case of incompressibility (Boussinesq approximation, see below), the two equations become identical.

Mechanical boundary condition: dynamic topography
Ricard et al. (2014)

- Free surface BC applied on the topography $z = h(x, y, t)$:

$$\boldsymbol{\sigma}(x, y, h(x, y, t), t) \cdot \hat{n} = \mathbf{0}. \tag{1}$$

- Hydrostatic balance nearly holds

$$\Rightarrow \tau = \mathcal{O}(\rho g h) \quad \text{and} \quad h = \mathcal{O}(\alpha \Delta T\, d).$$

$\Rightarrow$ develop linearly eq. (1):

$$\boldsymbol{\sigma}(x, y, 0, t) \cdot \hat{n} + \rho \boldsymbol{g} \cdot \hat{n} h(x, y, t) = \mathbf{0}. \tag{2}$$

- The slope of the topography is $\mathcal{O}(\alpha \Delta T d / L)$ with L the horizontal wavelength of convection. It is small enough that equation (2) can be simplified to

$$\sigma_{zz}(x, y, 0, t) = -\rho g h(x, y, t), \tag{3}$$

$$\tau_{zx}(x, y, 0, t) = \tau_{zx}(x, y, 0, t) = 0. \tag{4}$$

Mechanical boundary condition: dynamic topography
Ricard et al. (2014)

- Free surface BC applied on the topography $z = h(x, y, t)$:

$$\boldsymbol{\sigma}(x, y, h(x, y, t), t) \cdot \hat{n} = \mathbf{0}. \tag{1}$$

- Hydrostatic balance nearly holds

$$\Rightarrow \tau = \mathcal{O}(\rho g h) \quad \text{and} \quad h = \mathcal{O}(\alpha \Delta T\, d).$$

$\Rightarrow$ develop linearly eq. (1):

$$\boldsymbol{\sigma}(x, y, 0, t) \cdot \hat{n} + \rho \boldsymbol{g} \cdot \hat{n} h(x, y, t) = \mathbf{0}. \tag{2}$$

- The slope of the topography is $\mathcal{O}(\alpha \Delta T d / L)$ with L the horizontal wavelength of convection. It is small enough that equation (2) can be simplified to

$$\sigma_{zz}(x, y, 0, t) = -\rho g h(x, y, t), \tag{3}$$

$$\tau_{zx}(x, y, 0, t) = \tau_{zx}(x, y, 0, t) = 0. \tag{4}$$

Mechanical boundary condition: dynamic topography

Ricard et al. (2014)

- Free surface BC applied on the topography $z = h(x, y, t)$:

$$\boldsymbol{\sigma}(x, y, h(x, y, t), t) \cdot \hat{n} = \mathbf{0}. \tag{1}$$

- Hydrostatic balance nearly holds

$$\Rightarrow \tau = \mathcal{O}(\rho g h) \quad \text{and} \quad h = \mathcal{O}(\alpha \Delta T\, d).$$

$\Rightarrow$ develop linearly eq. (1):

$$\boldsymbol{\sigma}(x, y, 0, t) \cdot \hat{n} + \rho \boldsymbol{g} \cdot \hat{n} h(x, y, t) = \mathbf{0}. \tag{2}$$

- The slope of the topography is $\mathcal{O}(\alpha \Delta T d / L)$ with L the horizontal wavelength of convection. It is small enough that equation (2) can be simplified to

$$\sigma_{zz}(x, y, 0, t) = -\rho g h(x, y, t), \tag{3}$$

$$\tau_{zx}(x, y, 0, t) = \tau_{zx}(x, y, 0, t) = 0. \tag{4}$$

Mechanical boundary condition: dynamic topography
Ricard et al. (2014)

- Free surface BC applied on the topography $z = h(x, y, t)$:

$$\boldsymbol{\sigma}(x, y, h(x, y, t), t) \cdot \hat{n} = \mathbf{0}. \tag{1}$$

- Hydrostatic balance nearly holds

$$\Rightarrow \tau = \mathcal{O}(\rho g h) \quad \text{and} \quad h = \mathcal{O}(\alpha \Delta T\, d).$$

$\Rightarrow$ develop linearly eq. (1):

$$\boldsymbol{\sigma}(x, y, 0, t) \cdot \hat{n} + \rho \boldsymbol{g} \cdot \hat{n} h(x, y, t) = \mathbf{0}. \tag{2}$$

- The slope of the topography is $\mathcal{O}(\alpha \Delta T d/L)$ with L the horizontal wavelength of convection. It is small enough that equation (2) can be simplified to

$$\sigma_{zz}(x, y, 0, t) = -\rho g h(x, y, t), \tag{3}$$

$$\tau_{zx}(x, y, 0, t) = \tau_{zx}(x, y, 0, t) = 0. \tag{4}$$

Equation for the topography
Ricard et al. (2014)

- Kinematic definition of the topography, with $\boldsymbol{u}_h$ and w_h the horizontal and vertical components of velocity of the surface:

$$\frac{\partial h}{\partial t} + \boldsymbol{u}_h \cdot \boldsymbol{\nabla} h = w_h.$$

- Neglect ∇h and assume $w_h = u_z(x, y, 0, t)$

$$\Rightarrow \frac{\partial h}{\partial t} = u_z(x, y, 0, t)$$

- Difficulty: time scale for the evolution of the topography, $\tau_\eta = \eta/\rho g d = \mathcal{O}(3 \times 10^3\,\mathrm{yr})$ (post–glacial rebound) very short compared to mantle dynamics time scale.

$\Rightarrow$ Most numerical studies consider instantaneous adjustment of topography and use the free–slip BCs:

$$u_z(x, y, 0, t) = 0 \tag{5}$$

$$\tau_{zx}(x, y, 0, t) = \tau_{zx}(x, y, 0, t) = 0. \tag{6}$$

- Topography is removed from the problem but can be computed as an output by

$$\sigma_{zz}(x, y, 0, t) = -\rho g h(x, y, t).$$

- In experiments, non–deformable container implies no–slip BC: $\boldsymbol{u} = \boldsymbol{0}$.

Equation for the topography
Ricard et al. (2014)

- Kinematic definition of the topography, with $\boldsymbol{u}_h$ and w_h the horizontal and vertical components of velocity of the surface:

$$\frac{\partial h}{\partial t} + \boldsymbol{u}_h \cdot \boldsymbol{\nabla} h = w_h.$$

- Neglect ∇h and assume $w_h = u_z(x, y, 0, t)$

$$\Rightarrow \frac{\partial h}{\partial t} = u_z(x, y, 0, t)$$

- Difficulty: time scale for the evolution of the topography, $\tau_\eta = \eta/\rho g d = \mathcal{O}(3 \times 10^3 \text{ yr})$ (post–glacial rebound) very short compared to mantle dynamics time scale.

$\Rightarrow$ Most numerical studies consider instantaneous adjustment of topography and use the free–slip BCs:

$$u_z(x, y, 0, t) = 0 \tag{5}$$

$$\tau_{zx}(x, y, 0, t) = \tau_{zx}(x, y, 0, t) = 0. \tag{6}$$

- Topography is removed from the problem but can be computed as an output by

$$\sigma_{zz}(x, y, 0, t) = -\rho g h(x, y, t).$$

- In experiments, non–deformable container implies no–slip BC: $\boldsymbol{u} = \boldsymbol{0}$.

- Kinematic definition of the topography, with $\boldsymbol{u}_h$ and w_h the horizontal and vertical components of velocity of the surface:

$$\frac{\partial h}{\partial t} + \boldsymbol{u}_h \cdot \boldsymbol{\nabla} h = w_h.$$

- Neglect ∇h and assume $w_h = u_z(x, y, 0, t)$

$$\Rightarrow \frac{\partial h}{\partial t} = u_z(x, y, 0, t)$$

- Difficulty: time scale for the evolution of the topography, $\tau_\eta = \eta/\rho g d = \mathcal{O}(3 \times 10^3\,\text{yr})$ (post–glacial rebound) very short compared to mantle dynamics time scale.

$\Rightarrow$ Most numerical studies consider instantaneous adjustment of topography and use the free–slip BCs:

$$u_z(x, y, 0, t) = 0 \tag{5}$$

$$\tau_{zx}(x, y, 0, t) = \tau_{zx}(x, y, 0, t) = 0. \tag{6}$$

- Topography is removed from the problem but can be computed as an output by

$$\sigma_{zz}(x, y, 0, t) = -\rho g h(x, y, t).$$

- In experiments, non–deformable container implies no–slip BC: $\boldsymbol{u} = \boldsymbol{0}$.

- Kinematic definition of the topography, with $\boldsymbol{u}_h$ and w_h the horizontal and vertical components of velocity of the surface:

$$\frac{\partial h}{\partial t} + \boldsymbol{u}_h \cdot \boldsymbol{\nabla} h = w_h.$$

- Neglect ∇h and assume $w_h = u_z(x, y, 0, t)$

$$\Rightarrow \frac{\partial h}{\partial t} = u_z(x, y, 0, t)$$

- Difficulty: time scale for the evolution of the topography, $\tau_\eta = \eta / \rho g d = \mathcal{O}(3 \times 10^3 \text{ yr})$ (post–glacial rebound) very short compared to mantle dynamics time scale.

$\Rightarrow$ Most numerical studies consider instantaneous adjustment of topography and use the free–slip BCs:

$$u_z(x, y, 0, t) = 0 \quad (5)$$

$$\tau_{zx}(x, y, 0, t) = \tau_{zx}(x, y, 0, t) = 0. \quad (6)$$

- Topography is removed from the problem but can be computed as an output by

$$\sigma_{zz}(x, y, 0, t) = -\rho g h(x, y, t).$$

- In experiments, non–deformable container implies no–slip BC: $\boldsymbol{u} = \boldsymbol{0}$.

- Kinematic definition of the topography, with $\boldsymbol{u}_h$ and w_h the horizontal and vertical components of velocity of the surface:
$$\frac{\partial h}{\partial t} + \boldsymbol{u}_h \cdot \boldsymbol{\nabla} h = w_h.$$
- Neglect ∇h and assume $w_h = u_z(x, y, 0, t)$
$$\Rightarrow \frac{\partial h}{\partial t} = u_z(x, y, 0, t)$$
- Difficulty: time scale for the evolution of the topography, $\tau_\eta = \eta/\rho g d = \mathcal{O}(3 \times 10^3\,\mathrm{yr})$ (post–glacial rebound) very short compared to mantle dynamics time scale.

$\Rightarrow$ Most numerical studies consider instantaneous adjustment of topography and use the free–slip BCs:
$$u_z(x, y, 0, t) = 0 \tag{5}$$
$$\tau_{zx}(x, y, 0, t) = \tau_{zx}(x, y, 0, t) = 0. \tag{6}$$

- Topography is removed from the problem but can be computed as an output by
$$\sigma_{zz}(x, y, 0, t) = -\rho g h(x, y, t).$$
- In experiments, non–deformable container implies no–slip BC: $\boldsymbol{u} = \boldsymbol{0}$.

Equation for the topography
Ricard et al. (2014)

- Kinematic definition of the topography, with $\boldsymbol{u}_h$ and w_h the horizontal and vertical components of velocity of the surface:

$$\frac{\partial h}{\partial t} + \boldsymbol{u}_h \cdot \boldsymbol{\nabla} h = w_h.$$

- Neglect ∇h and assume $w_h = u_z(x, y, 0, t)$

$$\Rightarrow \frac{\partial h}{\partial t} = u_z(x, y, 0, t)$$

- Difficulty: time scale for the evolution of the topography, $\tau_\eta = \eta/\rho g d = \mathcal{O}(3 \times 10^3\ \text{yr})$ (post–glacial rebound) very short compared to mantle dynamics time scale.

$\Rightarrow$ Most numerical studies consider instantaneous adjustment of topography and use the free–slip BCs:

$$u_z(x, y, 0, t) = 0 \tag{5}$$

$$\tau_{zx}(x, y, 0, t) = \tau_{zx}(x, y, 0, t) = 0. \tag{6}$$

- Topography is removed from the problem but can be computed as an output by

$$\sigma_{zz}(x, y, 0, t) = -\rho g h(x, y, t).$$

- In experiments, non–deformable container implies no–slip BC: $\boldsymbol{u} = \boldsymbol{0}$.

Thermal boundary conditions

- Solids in contact with low viscosity fluids above and/or below that can be considered as well mixed: uniform temperature.
- Experiments: fluid in contact with a lid. Continuity of temperature and heat flux. In dimensionless form, it can be written as a Robin BC:

$$Bi\theta + \frac{\partial \theta}{\partial z} = 0$$

  with θ the temperature anomaly and Bi the Biot number.

  - $Bi \to \infty$: fixed temperature (Dirichlet BC)
  - $Bi \to 0$: fixed flux (Neumann BC)

  Reality is often in–between. May apply to the effect of continents on mantle convection (Grigné et al., 2007a,b).

Constitutive equations 1: Fourier's law

$$\boldsymbol{q} = -k\boldsymbol{\nabla}T$$

- Second principle:

$$\frac{-1}{T^2}\boldsymbol{q}\cdot\boldsymbol{\nabla}T = k\left(\frac{\boldsymbol{\nabla}T}{T}\right)^2 \geq 0 \Rightarrow k > 0$$

- Valid for a very wide range of materials and temperature gradients.
- For crystals, usually anisotropic:

$$\boldsymbol{q} = -\boldsymbol{k}\cdot\boldsymbol{\nabla}T \Leftrightarrow q_i = -k_{ij}\partial_j T$$

This is probably the case in the Earth's mantle where seismic anisotropy is measured.

- Second principle : eigenvalues of $\boldsymbol{k} > 0$

Constitutive equations 1: Fourier's law

$$\boldsymbol{q} = -k\boldsymbol{\nabla} T$$

- Second principle:
$$\frac{-1}{T^2}\boldsymbol{q}\cdot\boldsymbol{\nabla} T = k\left(\frac{\boldsymbol{\nabla} T}{T}\right)^2 \geq 0 \Rightarrow k > 0$$
- Valid for a very wide range of materials and temperature gradients.
- For crystals, usually anisotropic:
$$\boldsymbol{q} = -\boldsymbol{k}\cdot\boldsymbol{\nabla} T \Leftrightarrow q_i = -k_{ij}\partial_j T$$
This is probably the case in the Earth's mantle where seismic anisotropy is measured.
- Second principle : eigenvalues of $\boldsymbol{k} > 0$

Constitutive equations 2: Rheology I

- Total stress $\boldsymbol{\sigma}$ has to be related to the strain rate tensor, $\boldsymbol{e} = \frac{1}{2}(\boldsymbol{\nabla u} + \boldsymbol{\nabla u}^T) \equiv (\partial_j u_i + \partial_i u_j)/2$. Isolating the thermodynamic pressure, P:

$$\boldsymbol{\sigma} = -P\boldsymbol{I} + \boldsymbol{F}(\boldsymbol{e}).$$

- Define the $\overline{P} = \sigma_{kk}/3$, the average pressure, and $\boldsymbol{\tau}$, the deviatoric stress as

$$\boldsymbol{\sigma} = -\overline{P}\boldsymbol{I} + \boldsymbol{\tau}.$$

- Newtonian rheology: $\boldsymbol{F}$ is a linear function, i.e.

$$\sigma_{ij} = -P\delta_{ij} + c_{ijkl}e_{kl}.$$

- For an isotropic fluid (which is not the case of Earth's mantle, Pouilloux et al., 2007)

$$\sigma_{ij} = -P\delta_{ij} + \lambda e_{kk}\delta_{ij} + 2\eta e_{ij}.$$

Constitutive equations 2: Rheology I

- Total stress $\boldsymbol{\sigma}$ has to be related to the strain rate tensor, $\boldsymbol{e} = \frac{1}{2}(\boldsymbol{\nabla u} + \boldsymbol{\nabla u}^T) \equiv (\partial_j u_i + \partial_i u_j)/2$. Isolating the thermodynamic pressure, P:

$$\boldsymbol{\sigma} = -P\boldsymbol{I} + \boldsymbol{F}(\boldsymbol{e}).$$

- Define the $\overline{P} = \sigma_{kk}/3$, the average pressure, and $\boldsymbol{\tau}$, the deviatoric stress as

$$\boldsymbol{\sigma} = -\overline{P}\boldsymbol{I} + \boldsymbol{\tau}.$$

- Newtonian rheology: $\boldsymbol{F}$ is a linear function, i.e.

$$\sigma_{ij} = -P\delta_{ij} + c_{ijkl}e_{kl}.$$

- For an isotropic fluid (which is not the case of Earth's mantle, Pouilloux et al., 2007)

$$\sigma_{ij} = -P\delta_{ij} + \lambda e_{kk}\delta_{ij} + 2\eta e_{ij}.$$

Constitutive equations 2: Rheology I

- Total stress $\boldsymbol{\sigma}$ has to be related to the strain rate tensor, $\boldsymbol{e} = \frac{1}{2}(\boldsymbol{\nabla u} + \boldsymbol{\nabla u}^T) \equiv (\partial_j u_i + \partial_i u_j)/2$. Isolating the thermodynamic pressure, P:

$$\boldsymbol{\sigma} = -P\boldsymbol{I} + \boldsymbol{F}(\boldsymbol{e}).$$

- Define the $\overline{P} = \sigma_{kk}/3$, the average pressure, and $\boldsymbol{\tau}$, the deviatoric stress as

$$\boldsymbol{\sigma} = -\overline{P}\boldsymbol{I} + \boldsymbol{\tau}.$$

- Newtonian rheology: $\boldsymbol{F}$ is a linear function, i.e.

$$\sigma_{ij} = -P\delta_{ij} + c_{ijkl}e_{kl}.$$

- For an isotropic fluid (which is not the case of Earth's mantle, Pouilloux et al., 2007)

$$\sigma_{ij} = -P\delta_{ij} + \lambda e_{kk}\delta_{ij} + 2\eta e_{ij}.$$

Constitutive equations 2: Rheology I

- Total stress $\boldsymbol{\sigma}$ has to be related to the strain rate tensor, $\boldsymbol{e} = \frac{1}{2}(\boldsymbol{\nabla u} + \boldsymbol{\nabla u}^T) \equiv (\partial_j u_i + \partial_i u_j)/2$. Isolating the thermodynamic pressure, P:

$$\boldsymbol{\sigma} = -P\boldsymbol{I} + \boldsymbol{F}(\boldsymbol{e}).$$

- Define the $\overline{P} = \sigma_{kk}/3$, the average pressure, and $\boldsymbol{\tau}$, the deviatoric stress as

$$\boldsymbol{\sigma} = -\overline{P}\boldsymbol{I} + \boldsymbol{\tau}.$$

- Newtonian rheology: $\boldsymbol{F}$ is a linear function, i.e.

$$\sigma_{ij} = -P\delta_{ij} + c_{ijkl}e_{kl}.$$

- For an isotropic fluid (which is not the case of Earth's mantle, Pouilloux et al., 2007)

$$\sigma_{ij} = -P\delta_{ij} + \lambda e_{kk}\delta_{ij} + 2\eta e_{ij}.$$

- Considering the trace of tensors and the rest, one gets

$$\tau_{ij} = \eta \left(\frac{\partial u_i}{\partial x_j} + \frac{\partial u_j}{\partial x_i} - \frac{2}{3}\delta_{ij} \boldsymbol{\nabla} \cdot \boldsymbol{u} \right), \tag{7}$$

$$\overline{P} = P - \left(\lambda + \frac{2}{3}\eta \right) \boldsymbol{\nabla} \cdot \boldsymbol{u}. \tag{8}$$

- The bulk viscosity, $\zeta = \lambda + 2\eta/3$ is difficult to measure and usually assumed zero (Stokes hypothesis), which gives

$$\sigma_{ij} = -P\delta_{ij} + \eta \left(\frac{\partial u_i}{\partial x_j} + \frac{\partial u_j}{\partial x_i} - \frac{2}{3}\delta_{ij} \boldsymbol{\nabla} \cdot \boldsymbol{u} \right).$$

- Considering the trace of tensors and the rest, one gets

$$\tau_{ij} = \eta \left(\frac{\partial u_i}{\partial x_j} + \frac{\partial u_j}{\partial x_i} - \frac{2}{3}\delta_{ij}\boldsymbol{\nabla}\cdot\boldsymbol{u} \right), \tag{7}$$

$$\overline{P} = P - \left(\lambda + \frac{2}{3}\eta \right) \boldsymbol{\nabla}\cdot\boldsymbol{u}. \tag{8}$$

- The bulk viscosity, $\zeta = \lambda + 2\eta/3$ is difficult to measure and usually assumed zero (Stokes hypothesis), which gives

$$\sigma_{ij} = -P\delta_{ij} + \eta \left(\frac{\partial u_i}{\partial x_j} + \frac{\partial u_j}{\partial x_i} - \frac{2}{3}\delta_{ij}\boldsymbol{\nabla}\cdot\boldsymbol{u} \right).$$

- Origin of motion: change of density (ρ) with temperature (T).

$\Rightarrow$ Thermal expansion coefficient:

$$\alpha = -\frac{1}{\rho}\left(\frac{\partial \rho}{\partial T}\right)_P .$$

- Minimal (linear) equation:

$$\rho = \rho_0 \left[1 - \alpha\,(T - T_0)\right] .$$

- Effect of pressure

$$\rho = \rho_0 \left[1 - \alpha\,(T - T_0) + \frac{P - P_0}{K_T}\right]$$

Important but not leading order since pressure variation is dominated by the hydrostatic, i.e. in the direction of g. Not considered at first!

- Effect of composition: needs additional parameters such as the FeO mass fraction for the Earth mantle.

- Origin of motion: change of density (ρ) with temperature (T).

$\Rightarrow$ Thermal expansion coefficient:

$$\alpha = -\frac{1}{\rho}\left(\frac{\partial \rho}{\partial T}\right)_P .$$

- Minimal (linear) equation:

$$\rho = \rho_0 \left[1 - \alpha \left(T - T_0\right)\right] .$$

- Effect of pressure

$$\rho = \rho_0 \left[1 - \alpha \left(T - T_0\right) + \frac{P - P_0}{K_T}\right]$$

  Important but not leading order since pressure variation is dominated by the hydrostatic, i.e. in the direction of g. Not considered at first!

- Effect of composition: needs additional parameters such as the FeO mass fraction for the Earth mantle.

- Origin of motion: change of density (ρ) with temperature (T).

$\Rightarrow$ Thermal expansion coefficient:

$$\alpha = -\frac{1}{\rho}\left(\frac{\partial \rho}{\partial T}\right)_P .$$

- Minimal (linear) equation:

$$\rho = \rho_0 \left[1 - \alpha\left(T - T_0\right)\right] .$$

- Effect of pressure

$$\rho = \rho_0 \left[1 - \alpha\left(T - T_0\right) + \frac{P - P_0}{K_T}\right]$$

  Important but not leading order since pressure variation is dominated by the hydrostatic, i.e. in the direction of $\boldsymbol{g}$. Not considered at first!

- Effect of composition: needs additional parameters such as the FeO mass fraction for the Earth mantle.

The Oberbeck–Boussinesq approximation

- Boussinesq (1903) and Oberbeck (1879) propose to simplify the full equations by setting the density constant in all terms but the buoyancy term.
- At the same level of approximation (more on that later) the dissipation is negligible and $C_p = C_v \equiv C$.
- The minimal set of equations for convection are (neglecting internal heating for now)

$$\boldsymbol{\nabla} \cdot \boldsymbol{u} = 0, \tag{9}$$

$$\rho_0 \frac{\mathrm{D}\,\boldsymbol{u}}{\mathrm{D}t} = -\boldsymbol{\nabla} P + \rho \boldsymbol{g} + \eta \boldsymbol{\nabla}^2 \boldsymbol{u}, \tag{10}$$

$$\frac{\mathrm{D}\,T}{\mathrm{D}t} = \kappa \boldsymbol{\nabla}^2 T, \tag{11}$$

$$\rho = \rho_0 \left[1 - \alpha(T - T_0)\right], \tag{12}$$

- and boundary conditions.

Generalities

- The problem (the equations) always admit several solutions, notably a motionless steady conduction solution

$\Rightarrow$ What controls the onset of motion? The (in–)stability of the steady conduction solution.

- What forms do the solutions take with motion?

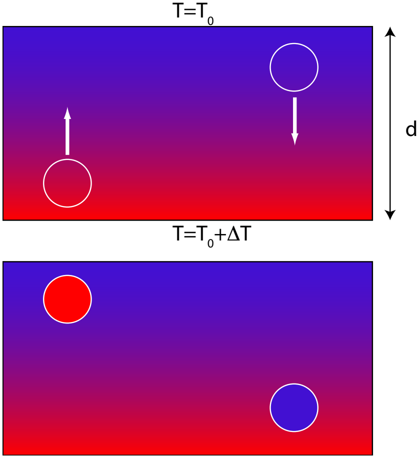

- Buoyancy: $\rho g \alpha \Delta T \sim \rho v/\tau_c \sim \rho d/\tau_c^2$.

$\Rightarrow$ Convective time: $\tau_c^2 = d/g\alpha\Delta T$.

- Diffusive time: $\tau_d = d^2/\kappa$.
- Viscous time: $\tau_v = d^2/\nu = \rho d^2/\eta$
- Convection if $\tau_v \tau_d/\tau_c^2 >> 1$

$$Ra \equiv \frac{\alpha \Delta T g d^3}{\kappa \nu} > R_c \sim 10^3$$

Gross estimate for Earth's mantle: $Ra \sim 10^8$

Dimensional analysis: the Rayleigh number

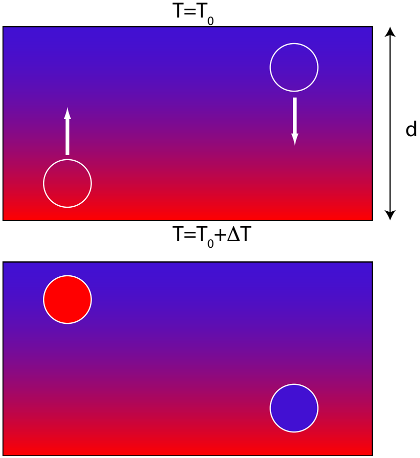

- Buoyancy: $\rho g \alpha \Delta T \sim \rho v/\tau_c \sim \rho d/\tau_c^2$.

$\Rightarrow$ Convective time: $\tau_c^2 = d/g\alpha\Delta T$.

- Diffusive time: $\tau_d = d^2/\kappa$.
- Viscous time: $\tau_v = d^2/\nu = \rho d^2/\eta$
- Convection if $\tau_v \tau_d/\tau_c^2 >> 1$

$$Ra \equiv \frac{\alpha \Delta T g d^3}{\kappa \nu} > R_c \sim 10^3$$

Gross estimate for Earth's mantle: $Ra \sim 10^8$

Dimensional analysis: the Rayleigh number

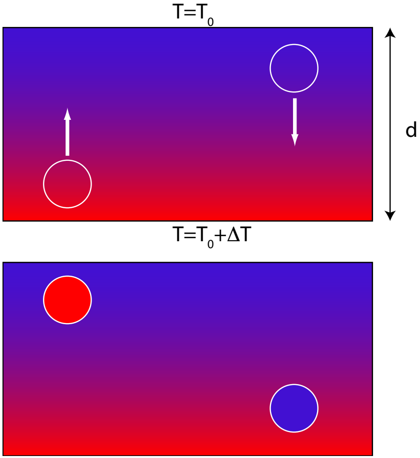

- Buoyancy: $\rho g \alpha \Delta T \sim \rho v/\tau_c \sim \rho d/\tau_c^2$.

$\Rightarrow$ Convective time: $\tau_c^2 = d/g\alpha\Delta T$.

- Diffusive time: $\tau_d = d^2/\kappa$.
- Viscous time: $\tau_v = d^2/\nu = \rho d^2/\eta$
- Convection if $\tau_v \tau_d/\tau_c^2 >> 1$

$$Ra \equiv \frac{\alpha \Delta T g d^3}{\kappa \nu} > R_c \sim 10^3$$

Gross estimate for Earth's mantle: $Ra \sim 10^8$

Dimensional analysis: the Rayleigh number

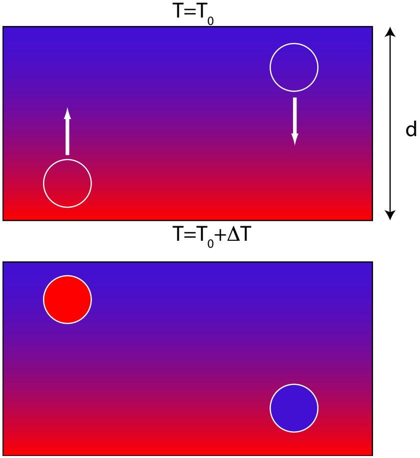

- Buoyancy: $\rho g \alpha \Delta T \sim \rho v/\tau_c \sim \rho d/\tau_c^2$.

$\Rightarrow$ Convective time: $\tau_c^2 = d/g\alpha\Delta T$.

- Diffusive time: $\tau_d = d^2/\kappa$.
- Viscous time: $\tau_v = d^2/\nu = \rho d^2/\eta$
- Convection if $\tau_v \tau_d/\tau_c^2 >> 1$

$$Ra \equiv \frac{\alpha \Delta T g d^3}{\kappa \nu} > R_c \sim 10^3$$

Gross estimate for Earth's mantle: $Ra \sim 10^8$

Perturbation equations

The system of equation admits a motionless ($\boldsymbol{u} = 0$) steady ($\partial_t = 0$) conduction solution:

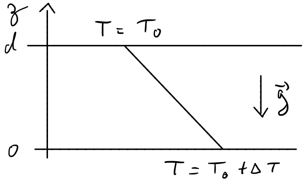

$$\boldsymbol{\nabla} P = \rho \boldsymbol{g} \tag{13}$$

$$\boldsymbol{\nabla}^2 T = 0 \tag{14}$$

$$\rho = \rho_0 \left[1 - \alpha(T - T_0)\right] \tag{15}$$

$$T(d) = T_0 \text{ and } T(0) = T_0 + \Delta T \tag{16}$$

$$\Rightarrow T_c = T_0 + \Delta T - \frac{z}{d} \Delta T \tag{17}$$

$$\rho_c = \rho_0 \left[1 - \alpha \Delta T \left(1 - \frac{z}{d}\right)\right] \Rightarrow P_c = \ldots \tag{18}$$

Write equations for the perturbations of the steady conduction solution, $\theta = T - T_c$, $p = P - P_c$:

$$\boldsymbol{\nabla} \cdot \boldsymbol{u} = 0 \tag{19}$$

$$\rho_0 \frac{\mathrm{D} \boldsymbol{u}}{\mathrm{D} t} = -\boldsymbol{\nabla} p - \rho_0 \alpha \theta \boldsymbol{g} + \eta \boldsymbol{\nabla}^2 \boldsymbol{u} \tag{20}$$

$$\frac{\mathrm{D} \theta}{\mathrm{D} t} = \frac{\Delta T}{d} u_z + \kappa \boldsymbol{\nabla}^2 \theta \tag{21}$$

- There are several ways of doing it but I choose here

$$x', y' = \frac{x, y}{d};\ z' = \frac{z}{d} + \frac{1}{2};\ \theta' = \frac{\theta}{\Delta T};\ t' = \frac{\kappa t}{d^2};\ p' = \frac{pd^2}{\kappa\eta}$$

- We get, after dropping the $'$s:

$$\nabla \cdot \boldsymbol{u} = 0 \tag{22}$$

$$\frac{1}{Pr}\frac{\mathrm{D}\boldsymbol{u}}{\mathrm{D}t} = -\nabla p + \nabla^2 \boldsymbol{u} + Ra\theta\hat{z} \tag{23}$$

$$\frac{\mathrm{D}\theta}{\mathrm{D}t} = u_z + \nabla^2\theta \tag{24}$$

- with

$$Ra = \frac{\rho_0 g\alpha\Delta T d^3}{\kappa\eta} \text{ the Rayleigh number} \tag{25}$$

$$Pr = \frac{\eta}{\rho_0\kappa} \text{ the Prandtl number} \tag{26}$$

- and boundary conditions at $z = \pm 1/2$ (free–slip for now)

$$\theta = 0;\ u_z = 0;\ \partial_z u_x = \partial_z u_y = 0 \Rightarrow \partial_z^2 u_z = 0.$$

- There are several ways of doing it but I choose here

$$x', y' = \frac{x, y}{d};\; z' = \frac{z}{d} + \frac{1}{2};\; \theta' = \frac{\theta}{\Delta T};\; t' = \frac{\kappa t}{d^2};\; p' = \frac{pd^2}{\kappa\eta}$$

- We get, after dropping the $'$s:

$$\nabla \cdot \boldsymbol{u} = 0 \tag{22}$$

$$\frac{1}{Pr}\frac{\mathrm{D}\boldsymbol{u}}{\mathrm{D}t} = -\nabla p + \nabla^2 \boldsymbol{u} + Ra\theta\hat{z} \tag{23}$$

$$\frac{\mathrm{D}\theta}{\mathrm{D}t} = u_z + \nabla^2\theta \tag{24}$$

- with

$$Ra = \frac{\rho_0 g\alpha\Delta T d^3}{\kappa\eta} \text{ the Rayleigh number} \tag{25}$$

$$Pr = \frac{\eta}{\rho_0\kappa} \text{ the Prandtl number} \tag{26}$$

- and boundary conditions at $z = \pm 1/2$ (free–slip for now)

$$\theta = 0;\; u_z = 0;\; \partial_z u_x = \partial_z u_y = 0 \Rightarrow \partial_z^2 u_z = 0.$$

Dimensionless equations

- There are several ways of doing it but I choose here

$$x', y' = \frac{x, y}{d};\ z' = \frac{z}{d} + \frac{1}{2};\ \theta' = \frac{\theta}{\Delta T};\ t' = \frac{\kappa t}{d^2};\ p' = \frac{pd^2}{\kappa\eta}$$

- We get, after dropping the $'$s:

$$\nabla \cdot \boldsymbol{u} = 0 \tag{22}$$

$$\frac{1}{Pr}\frac{\mathrm{D}\boldsymbol{u}}{\mathrm{D}t} = -\nabla p + \nabla^2 \boldsymbol{u} + Ra\theta\hat{z} \tag{23}$$

$$\frac{\mathrm{D}\theta}{\mathrm{D}t} = u_z + \nabla^2\theta \tag{24}$$

- with

$$Ra = \frac{\rho_0 g\alpha\Delta T d^3}{\kappa\eta} \text{ the Rayleigh number} \tag{25}$$

$$Pr = \frac{\eta}{\rho_0\kappa} \text{ the Prandtl number} \tag{26}$$

- and boundary conditions at $z = \pm 1/2$ (free–slip for now)

$$\theta = 0;\ u_z = 0;\ \partial_z u_x = \partial_z u_y = 0 \Rightarrow \partial_z^2 u_z = 0.$$

The Prandtl number

- Characteristics of the working fluid
- Liquid water: $Pr \sim 7$
- Earth's mantle: $Pr \sim 10^{25}$
- Water ice: $Pr \sim 10^{17}$

$\Rightarrow$ Inertia term negligible for convection in solids!

- Kinetic energy of Earth's mantle (mass 4×10^{24} kg), assuming a mean velocity of 3 cm/yr is $\sim 2 \times 10^{6}$ J. Similar to a car driving at 100 km/hr.

$\Rightarrow$ The Prandtl number is taken as infinite.

Mode decomposition for the linear problem I

- Considering infinitely small perturbations of the conduction solution, the problem can be linearised:

$$\nabla \cdot \boldsymbol{u} = 0 \tag{27}$$

$$\frac{1}{Pr}\frac{\partial \boldsymbol{u}}{\partial t} = -\nabla p + \nabla^2 \boldsymbol{u} + Ra\theta\hat{z} \tag{28}$$

$$\frac{\partial \theta}{\partial t} = u_z + \nabla^2 \theta \tag{29}$$

- The perturbation can be developed in time–dependent Fourier modes and, for a linear problem, each mode can be analysed independently. The problem is independent of the horizontal orientation and we choose:

$$(\theta, p, u_x, u_z) = (\Theta(z), P(z), U(z), W(z))\mathrm{e}^{\sigma t}\mathrm{e}^{\mathrm{i}kx}.$$

- If $\Re(\sigma) > 0$ the instability grows.
- The conduction solution is stable if *all* modes of perturbation have $\Re(\sigma) < 0$

Mode decomposition for the linear problem II

- Denoting $\mathsf{D} \equiv \frac{\mathrm{d}}{\mathrm{d}z}$

$$\mathrm{i}kU + \mathsf{D}\,W = 0, \tag{30}$$

$$\mathit{Pr}\left[-\mathrm{i}kP + \left(\mathsf{D}^2 - k^2\right)\,U\right] = \sigma\,U, \tag{31}$$

$$\mathit{Pr}\left[-\,\mathsf{D}P + \left(\mathsf{D}^2 - k^2\right)\,W + \mathit{Ra}\Theta\right] = \sigma\,W, \tag{32}$$

$$W + \left(\mathsf{D}^2 - k^2\right)\Theta = \sigma\Theta \tag{33}$$

- This is a generalised eigenvalue problem of the form:

$$\mathbf{L}\cdot\boldsymbol{X} = \sigma\mathbf{R}\cdot\boldsymbol{X} \tag{34}$$

with $\boldsymbol{X} = (P;\, U;\, W;\, \Theta)^T$ the global vertical mode and **R** a diagonal matrix with 0 or 1 on the diagonal.

- with boundary conditions for the free–slip case

$$W\left(\pm\frac{1}{2}\right) = 0;\;\; \mathsf{D}\,U\left(\pm\frac{1}{2}\right) = 0;\;\; \Theta\left(\pm\frac{1}{2}\right) = 0$$

- Define the dot product of two modes as

$$\langle \boldsymbol{X}_2 | \boldsymbol{X}_1 \rangle = \int \mathrm{e}^{\mathrm{i}(k_1 - k_2)x} \int_{-\frac{1}{2}}^{\frac{1}{2}} \left[\bar{P}_2 P1 + \bar{U}_2 U_1 + \bar{W}_2 W1 + Ra \bar{\Theta}_2 \Theta_1 \right] \mathrm{d}z \, \mathrm{d}x$$

  with $\bar{U}$ the complex–conjugate of U, etc.
- Then a series of integrations by part, using the boundary conditions, allows you to show (Schlüter et al., 1965) that

$$\langle \boldsymbol{X}_2 | \mathbf{L} \boldsymbol{X}_1 \rangle = \langle \mathbf{L} \boldsymbol{X}_2 | \boldsymbol{X}_1 \rangle$$

  meaning that the Linear problem is self–adjoint. The **R** operator is also self–adjoint.

$\Rightarrow$ All the eigenvalues are real:

$$\langle \boldsymbol{X} | \mathbf{L} \boldsymbol{X} \rangle = \langle \boldsymbol{X} | \sigma \mathbf{R} \boldsymbol{X} \rangle = \sigma \langle \boldsymbol{X} | \mathbf{R} \boldsymbol{X} \rangle$$
$$\langle \mathbf{L} \boldsymbol{X} | \boldsymbol{X} \rangle = \langle \sigma \mathbf{R} \boldsymbol{X} | \boldsymbol{X} \rangle = \bar{\sigma} \langle \mathbf{R} \boldsymbol{X} | \boldsymbol{X} \rangle$$

$$\Rightarrow \sigma = \Re(\sigma)$$

- The instability is characterised by the change of sign of σ. We just need to search for $\sigma = 0$ (neutral stability).

Solution for free–slip BCs

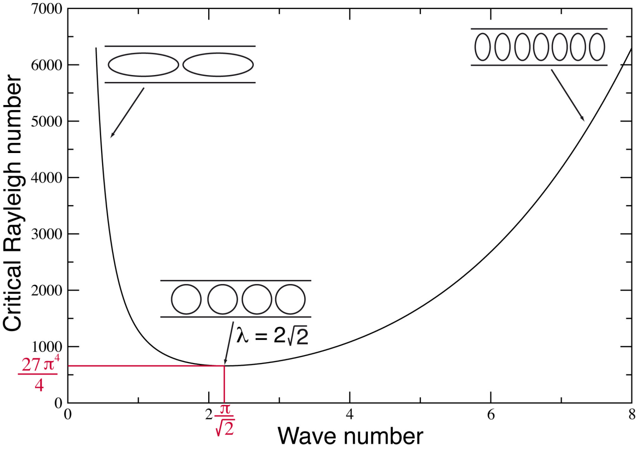

- First unstable mode has wavelength

$$\lambda_c = \frac{2\pi}{k_c} = 2\sqrt{2}.$$

$\Rightarrow$ rolls $\sqrt{2}$ wider than they are tall.

- When both boundaries are free–slip, $W = \cos(\pi z)$ provides the solution.
- Neutral stability:

$$Ra_c = \frac{\left(\pi^2 + k^2\right)^3}{k^2}$$

- Minimum value

$$R_c = \frac{27\pi^4}{4} \simeq 657 \text{ for } k_c = \frac{\pi}{\sqrt{2}}$$

Numerical technique for more general BCs

- Rigid BC: $u_z = u_x = 0$. Since $\partial_x u_x + \partial_z u_z = 0$, this implies that $\partial_z u_z = 0$ at the boundary.
- For at least one rigid BC, solution has to be computed numerically, for example by series expansion of the vertical mode.
- A simple way: use differentiation matrices with Chebyshev colocation pseudo-spectral method (e.g. Guo et al., 2012).
- A function $F(z)$ defined on $[-1, 1]$ is discretised on Chebyshev–Gauss–Lobatto nodal points $z_i = \cos(i\pi/N)$, for $i = 0..N$, to get vector $\boldsymbol{F} \equiv (F_i)_{i=0..N}$.
- The n^{th} derivative at the same points is simply obtained using the corresponding differentiation matrix $\mathbf{D}^{(n)}$:

$$\boldsymbol{F}^{(n)} = \mathbf{D}^{(n)} \cdot \boldsymbol{F}$$

- The linear operator $\mathbf{L}$ is written as a block matrix where the D operator is replaced by the differentiation matrix.
- Lines corresponding to the boundaries are replaced by corresponding BCs, with a 0 on the diagonal of $\mathbf{R}$, or simply removed for Dirichlet BCs.
- Use an eigenvector–eigenvalue solver (e.g. in Python) to find the eigenvalue as function of *Ra*. Differentiation matrices are available in Python at https://github.com/labrosse/dmsuite.
- Procedure:
  - For a given wavenumber k, find the value $Ra(k)$ that makes $\sigma = 0$.
  - Find the value of k that minimizes $Ra(k)$

Numerical technique for more general BCs

- Rigid BC: $u_z = u_x = 0$. Since $\partial_x u_x + \partial_z u_z = 0$, this implies that $\partial_z u_z = 0$ at the boundary.
- For at least one rigid BC, solution has to be computed numerically, for example by series expansion of the vertical mode.
- A simple way: use differentiation matrices with Chebyshev colocation pseudo-spectral method (e.g. Guo et al., 2012).
- A function $F(z)$ defined on $[-1, 1]$ is discretised on Chebyshev–Gauss–Lobatto nodal points $z_i = \cos(i\pi/N)$, for $i = 0..N$, to get vector $\boldsymbol{F} \equiv (F_i)_{i=0..N}$.
- The n^{th} derivative at the same points is simply obtained using the corresponding differentiation matrix $\mathbf{D}^{(n)}$:

$$\boldsymbol{F}^{(n)} = \mathbf{D}^{(n)} \cdot \boldsymbol{F}$$

- The linear operator $\mathbf{L}$ is written as a block matrix where the D operator is replaced by the differentiation matrix.
- Lines corresponding to the boundaries are replaced by corresponding BCs, with a 0 on the diagonal of $\mathbf{R}$, or simply removed for Dirichlet BCs.
- Use an eigenvector–eigenvalue solver (e.g. in Python) to find the eigenvalue as function of *Ra*. Differentiation matrices are available in Python at https://github.com/labrosse/dmsuite.
- Procedure:
  - For a given wavenumber k, find the value $Ra(k)$ that makes $\sigma = 0$.
  - Find the value of k that minimizes $Ra(k)$

- Rigid BC: $u_z = u_x = 0$. Since $\partial_x u_x + \partial_z u_z = 0$, this implies that $\partial_z u_z = 0$ at the boundary.
- For at least one rigid BC, solution has to be computed numerically, for example by series expansion of the vertical mode.
- A simple way: use differentiation matrices with Chebyshev colocation pseudo-spectral method (e.g. Guo et al., 2012).
- A function $F(z)$ defined on $[-1, 1]$ is discretised on Chebyshev–Gauss–Lobatto nodal points $z_i = \cos(i\pi/N)$, for $i = 0..N$, to get vector $\boldsymbol{F} \equiv (F_i)_{i=0..N}$.
- The n^{th} derivative at the same points is simply obtained using the corresponding differentiation matrix $\mathbf{D}^{(n)}$:

$$\boldsymbol{F}^{(n)} = \mathbf{D}^{(n)} \cdot \boldsymbol{F}$$

- The linear operator $\mathbf{L}$ is written as a block matrix where the D operator is replaced by the differentiation matrix.
- Lines corresponding to the boundaries are replaced by corresponding BCs, with a 0 on the diagonal of $\mathbf{R}$, or simply removed for Dirichlet BCs.
- Use an eigenvector–eigenvalue solver (e.g. in Python) to find the eigenvalue as function of *Ra*. Differentiation matrices are available in Python at https://github.com/labrosse/dmsuite.
- Procedure:
  - For a given wavenumber k, find the value $Ra(k)$ that makes $\sigma = 0$.
  - Find the value of k that minimizes $Ra(k)$

Numerical technique for more general BCs

- Rigid BC: $u_z = u_x = 0$. Since $\partial_x u_x + \partial_z u_z = 0$, this implies that $\partial_z u_z = 0$ at the boundary.
- For at least one rigid BC, solution has to be computed numerically, for example by series expansion of the vertical mode.
- A simple way: use differentiation matrices with Chebyshev colocation pseudo-spectral method (e.g. Guo et al., 2012).
- A function $F(z)$ defined on $[-1, 1]$ is discretised on Chebyshev–Gauss–Lobatto nodal points $z_i = \cos(i\pi/N)$, for $i = 0..N$, to get vector $\boldsymbol{F} \equiv (F_i)_{i=0..N}$.
- The n^{th} derivative at the same points is simply obtained using the corresponding differentiation matrix $\mathbf{D}^{(n)}$:

$$\boldsymbol{F}^{(n)} = \mathbf{D}^{(n)} \cdot \boldsymbol{F}$$

- The linear operator $\mathbf{L}$ is written as a block matrix where the D operator is replaced by the differentiation matrix.
- Lines corresponding to the boundaries are replaced by corresponding BCs, with a 0 on the diagonal of $\mathbf{R}$, or simply removed for Dirichlet BCs.
- Use an eigenvector–eigenvalue solver (e.g. in Python) to find the eigenvalue as function of *Ra*. Differentiation matrices are available in Python at https://github.com/labrosse/dmsuite.
- Procedure:
  - For a given wavenumber k, find the value $Ra(k)$ that makes $\sigma = 0$.
  - Find the value of k that minimizes $Ra(k)$

Numerical technique for more general BCs

- Rigid BC: $u_z = u_x = 0$. Since $\partial_x u_x + \partial_z u_z = 0$, this implies that $\partial_z u_z = 0$ at the boundary.
- For at least one rigid BC, solution has to be computed numerically, for example by series expansion of the vertical mode.
- A simple way: use differentiation matrices with Chebyshev colocation pseudo-spectral method (e.g. Guo et al., 2012).
- A function $F(z)$ defined on $[-1, 1]$ is discretised on Chebyshev–Gauss–Lobatto nodal points $z_i = \cos(i\pi/N)$, for $i = 0..N$, to get vector $\boldsymbol{F} \equiv (F_i)_{i=0..N}$.
- The n^{th} derivative at the same points is simply obtained using the corresponding differentiation matrix $\mathbf{D}^{(n)}$:

$$\boldsymbol{F}^{(n)} = \mathbf{D}^{(n)} \cdot \boldsymbol{F}$$

- The linear operator $\mathbf{L}$ is written as a block matrix where the D operator is replaced by the differentiation matrix.
- Lines corresponding to the boundaries are replaced by corresponding BCs, with a 0 on the diagonal of $\mathbf{R}$, or simply removed for Dirichlet BCs.
- Use an eigenvector–eigenvalue solver (e.g. in Python) to find the eigenvalue as function of *Ra*. Differentiation matrices are available in Python at https://github.com/labrosse/dmsuite.
- Procedure:
  - For a given wavenumber k, find the value $Ra(k)$ that makes $\sigma = 0$.
  - Find the value of k that minimizes $Ra(k)$

Numerical technique for more general BCs

- Rigid BC: $u_z = u_x = 0$. Since $\partial_x u_x + \partial_z u_z = 0$, this implies that $\partial_z u_z = 0$ at the boundary.
- For at least one rigid BC, solution has to be computed numerically, for example by series expansion of the vertical mode.
- A simple way: use differentiation matrices with Chebyshev colocation pseudo-spectral method (e.g. Guo et al., 2012).
- A function $F(z)$ defined on $[-1, 1]$ is discretised on Chebyshev–Gauss–Lobatto nodal points $z_i = \cos(i\pi/N)$, for $i = 0..N$, to get vector $\boldsymbol{F} \equiv (F_i)_{i=0..N}$.
- The n^{th} derivative at the same points is simply obtained using the corresponding differentiation matrix $\mathbf{D}^{(n)}$:

$$\boldsymbol{F}^{(n)} = \mathbf{D}^{(n)} \cdot \boldsymbol{F}$$

- The linear operator $\mathbf{L}$ is written as a block matrix where the D operator is replaced by the differentiation matrix.
- Lines corresponding to the boundaries are replaced by corresponding BCs, with a 0 on the diagonal of $\mathbf{R}$, or simply removed for Dirichlet BCs.
- Use an eigenvector–eigenvalue solver (e.g. in Python) to find the eigenvalue as function of *Ra*. Differentiation matrices are available in Python at https://github.com/labrosse/dmsuite.
- Procedure:
  - For a given wavenumber k, find the value $Ra(k)$ that makes $\sigma = 0$.
  - Find the value of k that minimizes $Ra(k)$

Numerical technique for more general BCs

- Rigid BC: $u_z = u_x = 0$. Since $\partial_x u_x + \partial_z u_z = 0$, this implies that $\partial_z u_z = 0$ at the boundary.
- For at least one rigid BC, solution has to be computed numerically, for example by series expansion of the vertical mode.
- A simple way: use differentiation matrices with Chebyshev colocation pseudo-spectral method (e.g. Guo et al., 2012).
- A function $F(z)$ defined on $[-1, 1]$ is discretised on Chebyshev–Gauss–Lobatto nodal points $z_i = \cos(i\pi/N)$, for $i = 0..N$, to get vector $\boldsymbol{F} \equiv (F_i)_{i=0..N}$.
- The n^{th} derivative at the same points is simply obtained using the corresponding differentiation matrix $\mathbf{D}^{(n)}$:

$$\boldsymbol{F}^{(n)} = \mathbf{D}^{(n)} \cdot \boldsymbol{F}$$

- The linear operator **L** is written as a block matrix where the D operator is replaced by the differentiation matrix.
- Lines corresponding to the boundaries are replaced by corresponding BCs, with a 0 on the diagonal of **R**, or simply removed for Dirichlet BCs.
- Use an eigenvector–eigenvalue solver (e.g. in Python) to find the eigenvalue as function of *Ra*. Differentiation matrices are available in Python at https://github.com/labrosse/dmsuite.
- Procedure:
  - For a given wavenumber k, find the value $Ra(k)$ that makes $\sigma = 0$.
  - Find the value of k that minimizes $Ra(k)$

Numerical technique for more general BCs

- Rigid BC: $u_z = u_x = 0$. Since $\partial_x u_x + \partial_z u_z = 0$, this implies that $\partial_z u_z = 0$ at the boundary.
- For at least one rigid BC, solution has to be computed numerically, for example by series expansion of the vertical mode.
- A simple way: use differentiation matrices with Chebyshev colocation pseudo-spectral method (e.g. Guo et al., 2012).
- A function $F(z)$ defined on $[-1, 1]$ is discretised on Chebyshev–Gauss–Lobatto nodal points $z_i = \cos(i\pi/N)$, for $i = 0..N$, to get vector $\boldsymbol{F} \equiv (F_i)_{i=0..N}$.
- The n^{th} derivative at the same points is simply obtained using the corresponding differentiation matrix $\mathbf{D}^{(n)}$:

$$\boldsymbol{F}^{(n)} = \mathbf{D}^{(n)} \cdot \boldsymbol{F}$$

- The linear operator **L** is written as a block matrix where the D operator is replaced by the differentiation matrix.
- Lines corresponding to the boundaries are replaced by corresponding BCs, with a 0 on the diagonal of **R**, or simply removed for Dirichlet BCs.
- Use an eigenvector–eigenvalue solver (e.g. in Python) to find the eigenvalue as function of *Ra*. Differentiation matrices are available in Python at https://github.com/labrosse/dmsuite.
- Procedure:
  - For a given wavenumber k, find the value *Ra*(k) that makes $\sigma = 0$.
  - Find the value of k that minimizes *Ra*(k)

Numerical technique for more general BCs

- Rigid BC: $u_z = u_x = 0$. Since $\partial_x u_x + \partial_z u_z = 0$, this implies that $\partial_z u_z = 0$ at the boundary.
- For at least one rigid BC, solution has to be computed numerically, for example by series expansion of the vertical mode.
- A simple way: use differentiation matrices with Chebyshev colocation pseudo-spectral method (e.g. Guo et al., 2012).
- A function $F(z)$ defined on $[-1, 1]$ is discretised on Chebyshev–Gauss–Lobatto nodal points $z_i = \cos(i\pi/N)$, for $i = 0..N$, to get vector $\boldsymbol{F} \equiv (F_i)_{i=0..N}$.
- The n^{th} derivative at the same points is simply obtained using the corresponding differentiation matrix $\mathbf{D}^{(n)}$:

$$\boldsymbol{F}^{(n)} = \mathbf{D}^{(n)} \cdot \boldsymbol{F}$$

- The linear operator **L** is written as a block matrix where the D operator is replaced by the differentiation matrix.
- Lines corresponding to the boundaries are replaced by corresponding BCs, with a 0 on the diagonal of **R**, or simply removed for Dirichlet BCs.
- Use an eigenvector–eigenvalue solver (e.g. in Python) to find the eigenvalue as function of *Ra*. Differentiation matrices are available in Python at https://github.com/labrosse/dmsuite.
- Procedure:
  - For a given wavenumber k, find the value *Ra*(k) that makes $\sigma = 0$.
  - Find the value of k that minimizes *Ra*(k)

$$\mathbf{L} = \begin{array}{cccccc} 0:N & 0:N & 0:N & 1:N-1 & \\ \left(\begin{array}{cccc} \mathbf{0} & \mathrm{i}k\mathbf{I} & \mathbf{D} & \mathbf{0} \\ \mathbf{0} & \mathbf{D} & \mathbf{0} & \mathbf{0} \\ -\mathit{Pr}\,\mathrm{i}k\mathbf{I} & \mathit{Pr}\left(\mathbf{D}^{(2)} - k^2\mathbf{I}\right) & \mathbf{0} & \mathbf{0} \\ \mathbf{0} & \mathbf{D} & \mathbf{0} & \mathbf{0} \\ -\mathit{Pr}\mathbf{D} & \mathbf{0} & \mathit{Pr}\left(\mathbf{D}^{(2)} - k^2\mathbf{I}\right) & \mathit{Pr}\,\mathit{Ra}\mathbf{I} \\ \mathbf{0} & \mathbf{0} & \mathbf{I} & \left(\mathbf{D}^{(2)} - k^2\mathbf{I}\right) \end{array}\right) & \begin{array}{l} 0:N \\ 0 \\ 1:N-1 \\ N \\ 1:N-1 \\ 1:N-1 \end{array} \end{array}$$

applies to vector $\boldsymbol{X} = (\boldsymbol{P}, \boldsymbol{U}, \boldsymbol{W}, \boldsymbol{\Theta})^T$ as

$$\mathbf{L} \cdot \boldsymbol{X} = \sigma \mathbf{R} \cdot \boldsymbol{X}.$$

- For infinite *Pr*, divide the velocity equations by *Pr* and make the corresponding diagonal values of **R** zero.
- Filter out infinite eigenvalues that are due to the zeros on the diagonal of **R**.

Effect of mechanical BCs on the linear stability

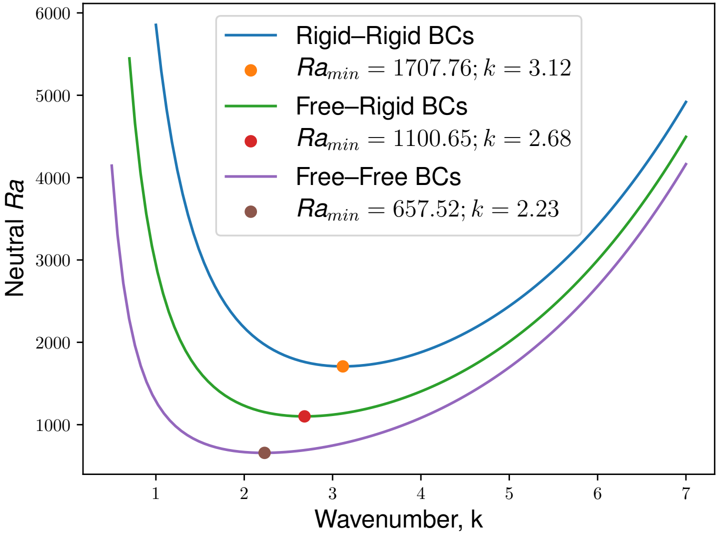

- A method pioneered by Malkus and Veronis (1958) for free-slip BCs and Schlüter et al. (1965) for rigid BCs. See also Manneville (2004).
- The conservation equations are split in their linear and non-linear parts:

$$\mathbf{L}(\partial_t, \partial_x, \partial_z, Ra)\boldsymbol{X} = \mathbf{N}(\boldsymbol{X}, \boldsymbol{X}), \tag{35}$$

  with $\boldsymbol{X} = (p; u; w; \theta)^T$. The linear operator is further developed around the critical Rayleigh number as

$$\mathbf{L} = \mathbf{L}_c - (Ra - Ra_c)\mathbf{M}. \tag{36}$$

The solution $\boldsymbol{X}$ and the Rayleigh number are developed as

$$\boldsymbol{X} = \epsilon \boldsymbol{X}_1 + \epsilon^2 \boldsymbol{X}_2 + \epsilon^3 \boldsymbol{X}_3 + \ldots \tag{37}$$

$$Ra = Ra_c + \epsilon Ra_1 + \epsilon^2 Ra_2 + \ldots \tag{38}$$

and we get a set of equations for the increasing order of ϵ:

$$\mathbf{L}_c \boldsymbol{X}_1 = \mathbf{0}, \tag{39}$$

$$\mathbf{L}_c \boldsymbol{X}_2 = \mathbf{N}(\boldsymbol{X}_1, \boldsymbol{X}_1) + Ra_1 \mathbf{M} \boldsymbol{X}_1, \tag{40}$$

$$\mathbf{L}_c \boldsymbol{X}_3 = \mathbf{N}(\boldsymbol{X}_1, \boldsymbol{X}_2) + \mathbf{N}(\boldsymbol{X}_2, \boldsymbol{X}_1) + Ra_1 \mathbf{M} \boldsymbol{X}_2 + Ra_2 \mathbf{M} \boldsymbol{X}_1. \tag{41}$$

$$\mathbf{L}_c \boldsymbol{X}_n = \sum_{l=1}^{n-1} \mathbf{N}(\boldsymbol{X}_l, \boldsymbol{X}_{n-l}) + \sum_{l=1}^{n-1} Ra_l \mathbf{M} \boldsymbol{X}_{n-l} \tag{42}$$

- Solvability condition for each degree obtained by taking the dot product by $\boldsymbol{X}_c$ and using the Hermitian property $\Rightarrow$ values of Ra_i.
- We can prove (Labrosse et al., 2018) that $Ra_{2n+1} = 0$ so that, to leading order,

$$\epsilon = \sqrt{\frac{Ra - Ra_c}{Ra_2}}, \tag{43}$$

$$Nu = 1 + A \frac{Ra - Ra_c}{Ra_c}, \tag{44}$$

  with $Nu = qd/k\Delta T$ the Nusselt number, the dimensionless heat flux.
- In the case of free-slip boundary conditions, the coefficient $A = 2$ can be determined analytically.

Stability of finite amplitude solutions

- Schlüter et al. (1965) showed that only rolls are stable finite amplitude solutions close to the onset of convection.
- Busse (1967) showed that a finite range of wavenumber leads to stable roll solution.

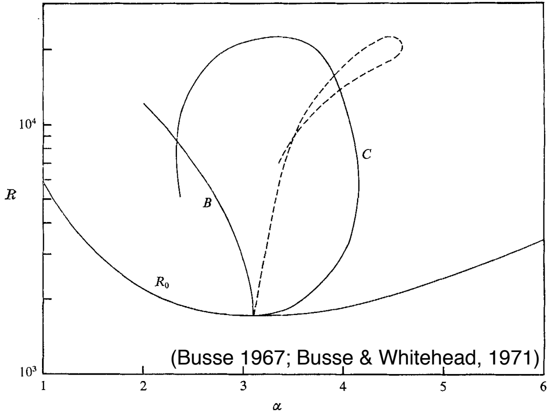

FIGURE 1. Stability region of convection rolls. The zigzag instability and the cross-roll instability produce the stability boundaries B and C, respectively. The dashed line denotes the value of the wave-number $\tilde{\alpha}$ of the marginal cross-roll disturbances along curve C.

Example calculation close to onset

- $\mathit{Ra} = 800, \ \mathit{Pr} = \infty$.
- Aspect ratio $= 32 \times 32 \times 1$.
- Initial condition: conductive solution plus random noise.
- Pattern dynamics with long–distance interactions between defects.
- Steady–state: Rolls at $\pi/4$ angle so that a natural number of $2\sqrt{2}$ wavelength fit.
- Method of solution: finite differences and multigrid (Sotin and Labrosse, 1999).

(Busse & Whitehead, 1971)

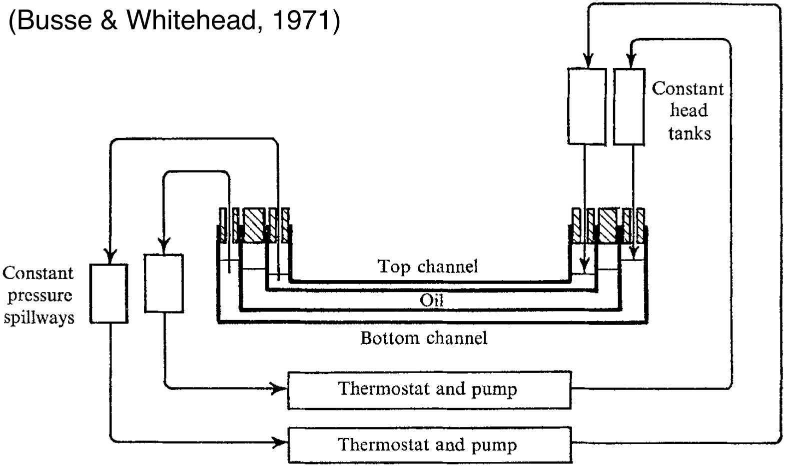

FIGURE 4. Schematic diagram of the experimental apparatus. Arrows indicate water flow, heavy black lines indicate glass, hashed regions indicate styrofoam insulation.

Experimental test of Busse (1967)'s theory

Busse and Whitehead (1971)

(Busse & Whitehead, 1971)

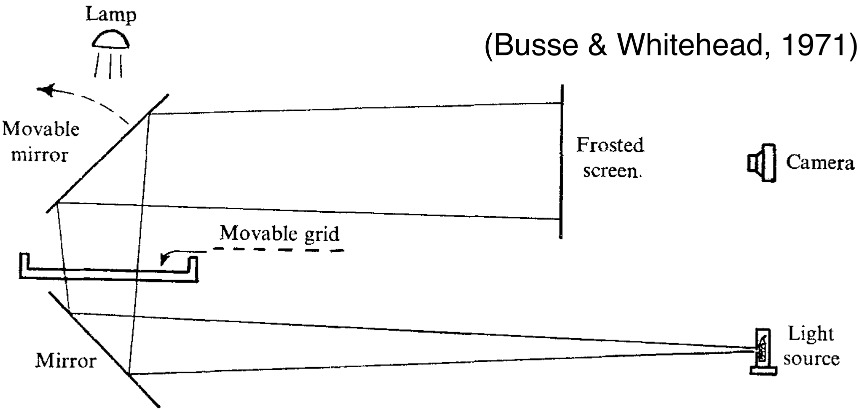

FIGURE 5. Diagram of the observational technique showing movable upper mirror and grid used for inducing rolls.

Experimental test of Busse (1967)'s theory

Busse and Whitehead (1971)

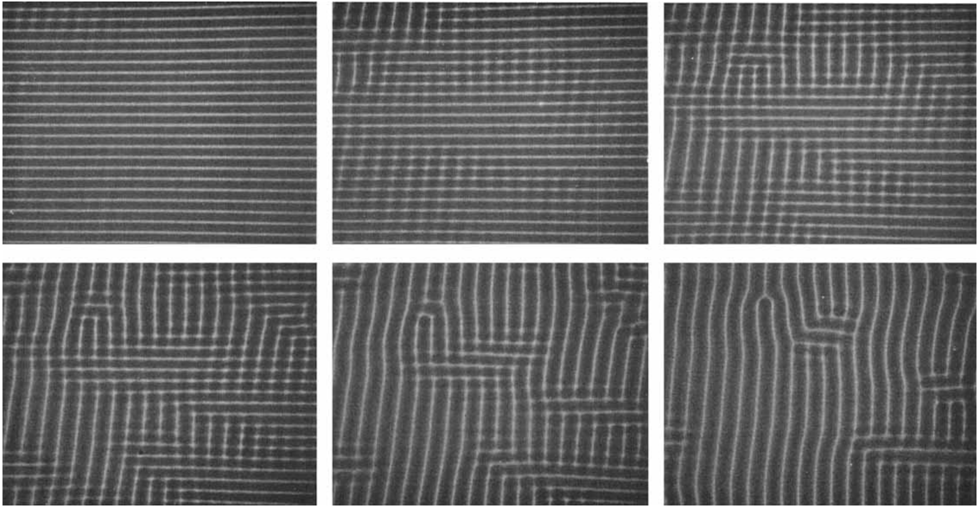

Fig. 10: Cross-roll instability at R=3000, d=5 mm, $\alpha=2\pi/1.64$.Time intervals between subsequent photographs are 10, 4, 3, 7 and 28 min, respectively.

Experimental test of Busse (1967)'s theory
Busse and Whitehead (1971)

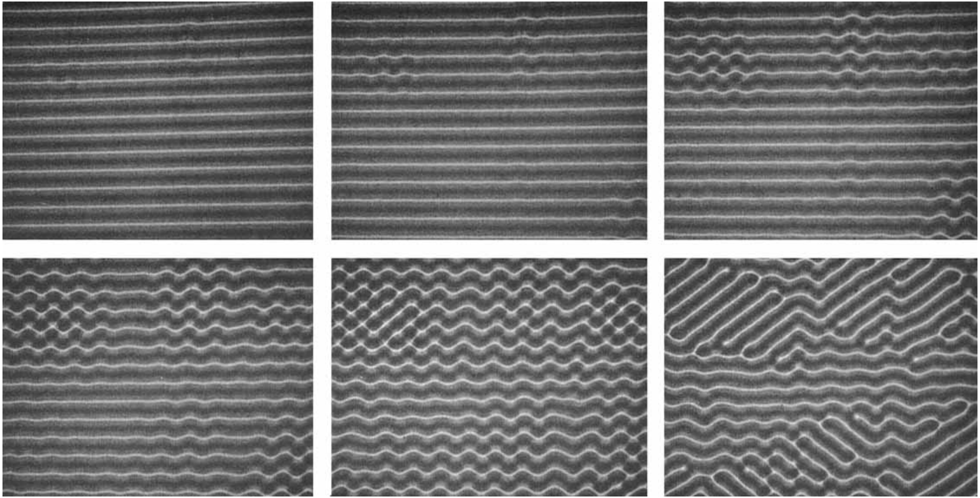

Fig. 11: Zigzag instability at R=3600, d=5 mm, $\alpha=2\pi/2.8$.Time intervals between subsequent photographs are 9, 10, 10, 26 and 72 min, respectively.
(Busse & Whitehead, 1971)

Experimental test of Busse (1967)'s theory

Busse and Whitehead (1971)

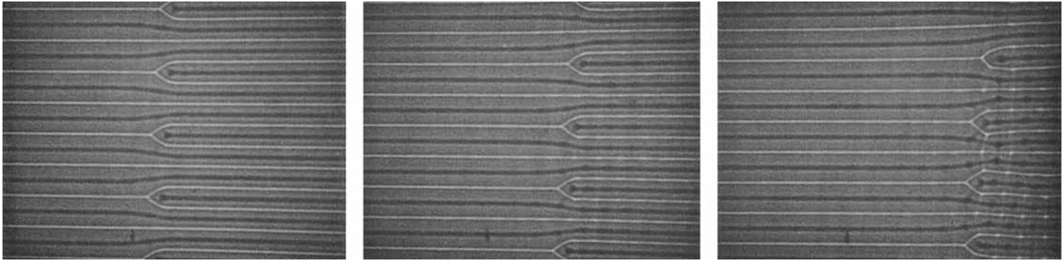

Fig. 15: Pinching instability at R=18x10^3, d=1 cm, α_1=2π/2.55, α_1=2π/1.7.
Time intervals between the photographs is 35 min. (Busse & Whitehead, 1971)

Experiments vs. theory of Busse balloon

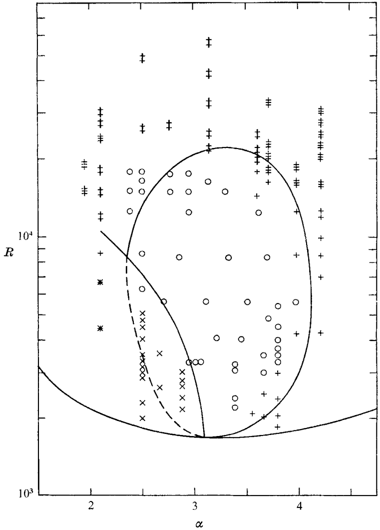

FIGURE 6. Experimental results. ○, stable rolls; ×, zigzag instability; +, cross-roll instability leading to rolls; ǂ, cross-roll instability leading to bimodal convection; ǂ, cross-roll instability inducing transient rolls with subsequent local processes. The curves correspond to the theoretical results shown in figure 1.

- Very good match of observations to the theory!

- Many experiments (starting with Bénard's) lead to hexagonal patterns.
- Hexagonal patterns are non–symmetrical with respect to $z \to -z$ tranformation, whereas rolls are.
- Hexagonal flow is obtained for asymmetrical conditions such as provided by depth– or temperature–dependent properties (e.g. $\eta(T)$) or volumetric heat generation (figure).

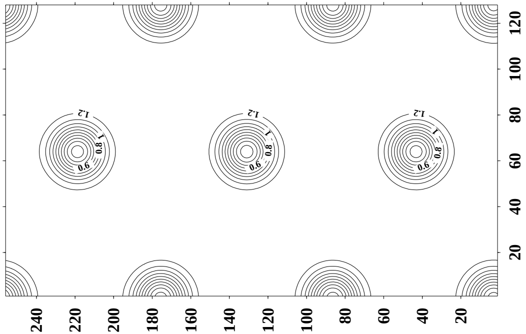

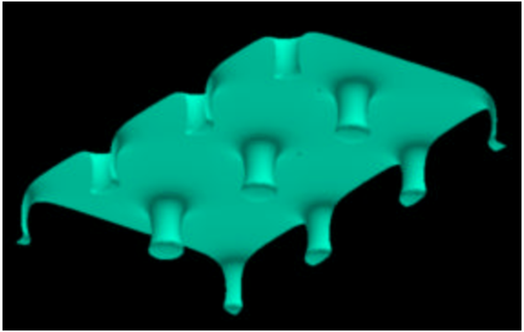

Example calculation at high *Ra*

- *Ra* $= 10^7$, *Pr* $= \infty$, aspect ratio $4 \times 4 \times 1$
- Initial conditions: $T = 1/2$ and exponential variation in thin layers to match BCs plus small random noise.
- Two iso-temperature surface represented.

Regime diagram in the (Ra, Pr) space

Krishnamurti (1973)

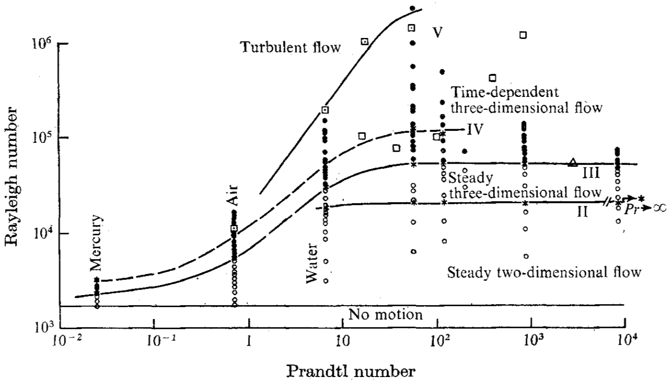

FIGURE 4. Regime diagram. ○, steady flows; ●, time-dependent flows; ★, transition points with observed change in slope; □, Rossby's observations of time-dependent flow; ⊡, Willis & Deardorff's (1967*a*) observations for turbulent flow; △, Silveston's point of transition for time-dependent flow (see text). (Krishnamurti, 1973)

$Ra = 10^7$

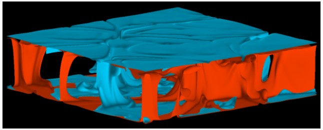

$Ra = 10^5$

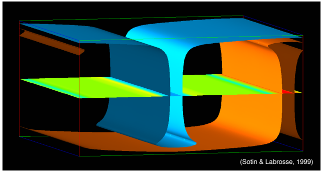

Temperature profiles

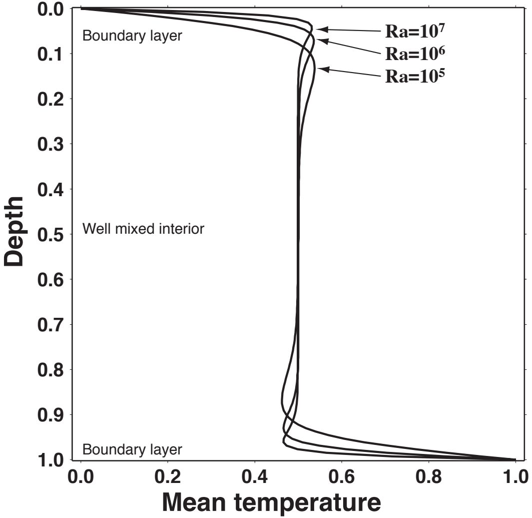

- Efficient mixing in the bulk of the domain $\Rightarrow$ uniform temperature.
- Matching the boundary conditions $\Rightarrow$ boundary layers.
- Increasing the Rayleigh number makes the thickness of boundary layers decrease.

Advection and conduction profiles

- Integrate the energy balance equation between the top boundary and any depth z, averaged over time:

$$q_{top} \equiv -\frac{\partial \overline{T}}{\partial z}\left(z=\frac{1}{2}\right) = -\frac{\partial \overline{T}}{\partial z}(z) + \overline{u_z(T(z)-\overline{T})}.$$

- Increase of velocity with *Ra* makes the advection increase $\Rightarrow$ thickness of boundary layers decreases to match the heat flow.

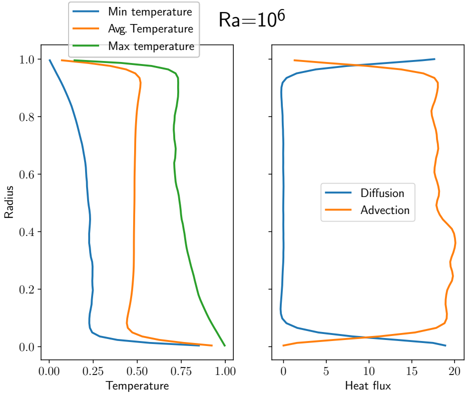

Simple dimensional argument for the heat flow

- Dimensionless heat flow $Nu = qd/k\Delta T = f(Ra) = ARa^{\beta}$ to be valid over large range of Ra values.
- At very large Ra, boundary layers and the resulting plumes get very small.
- The dynamics of convection and the resulting heat flow should become independent of the total thickness:

$$q = A\frac{k\Delta T}{d}\left(\frac{g\alpha\Delta T d^3}{\kappa\nu}\right)^{\beta} \Rightarrow \beta = \frac{1}{3}.$$

Boundary layer instabilities

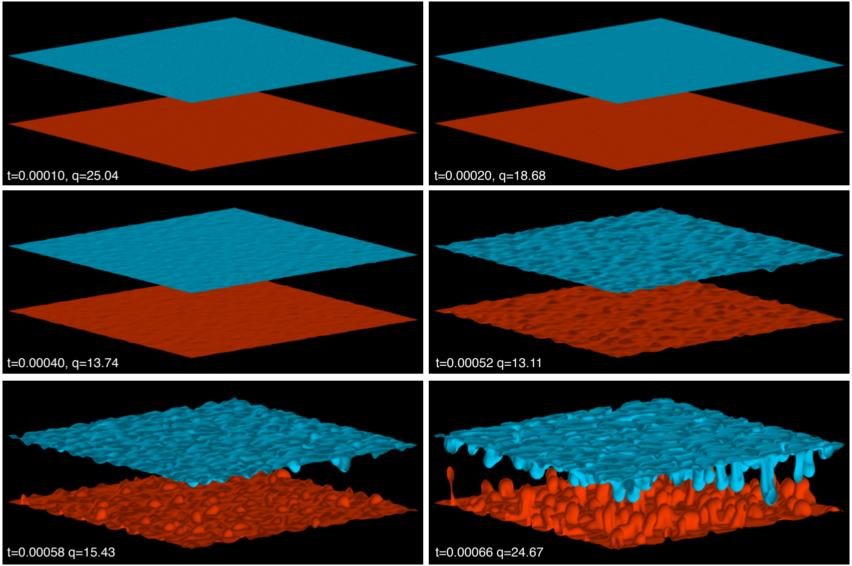

Howard (1964) proposed a simple model for convection at high *Ra*:

- Based on observations of boundary layers (BL) instabilities.
- Boundary layer grows by diffusion.
- BL becomes unstable when its Rayleigh number reaches a critical value.
- Cycle restarts.
- Ergodicity assumptions: horizontal average on an infinite layer equals time average on one cycle.
- Diffusive part of the cycle takes much longer than destabilisation part $\Rightarrow$ dominates the time average.

$$\Rightarrow \overline{T} = \frac{1}{t_c}\int_0^{t_c} \frac{\Delta T}{2}\,\mathrm{erf}\left(\frac{0.5-z}{2\sqrt{\kappa t}}\right)\mathrm{d}t$$

  for the top boundary layer and something equivalent at the bottom.
- Heat flux

$$\overline{q} = \frac{1}{t_c}\int_0^{t_c} \frac{k\Delta T}{2\sqrt{\pi\kappa t}}\,\mathrm{d}t = \frac{k\Delta T}{\sqrt{\pi\kappa t_c}} = \frac{k\Delta T}{\delta_c}.$$

Howard's model I

Howard (1964) proposed a simple model for convection at high *Ra*:

- Based on observations of boundary layers (BL) instabilities.
- Boundary layer grows by diffusion.
- BL becomes unstable when its Rayleigh number reaches a critical value.
- Cycle restarts.
- Ergodicity assumptions: horizontal average on an infinite layer equals time average on one cycle.
- Diffusive part of the cycle takes much longer than destabilisation part $\Rightarrow$ dominates the time average.

$$\Rightarrow \overline{T} = \frac{1}{t_c}\int_0^{t_c} \frac{\Delta T}{2}\,\mathrm{erf}\left(\frac{0.5-z}{2\sqrt{\kappa t}}\right)\mathrm{d}t$$

  for the top boundary layer and something equivalent at the bottom.
- Heat flux

$$\overline{q} = \frac{1}{t_c}\int_0^{t_c} \frac{k\Delta T}{2\sqrt{\pi\kappa t}}\,\mathrm{d}t = \frac{k\Delta T}{\sqrt{\pi\kappa t_c}} = \frac{k\Delta T}{\delta_c}.$$

Howard (1964) proposed a simple model for convection at high *Ra*:

- Based on observations of boundary layers (BL) instabilities.
- Boundary layer grows by diffusion.
- BL becomes unstable when its Rayleigh number reaches a critical value.
- Cycle restarts.
- Ergodicity assumptions: horizontal average on an infinite layer equals time average on one cycle.
- Diffusive part of the cycle takes much longer than destabilisation part $\Rightarrow$ dominates the time average.

$$\Rightarrow \overline{T} = \frac{1}{t_c}\int_0^{t_c} \frac{\Delta T}{2}\,\mathrm{erf}\left(\frac{0.5-z}{2\sqrt{\kappa t}}\right)\mathrm{d}t$$

  for the top boundary layer and something equivalent at the bottom.
- Heat flux

$$\overline{q} = \frac{1}{t_c}\int_0^{t_c}\frac{k\Delta T}{2\sqrt{\pi\kappa t}}\,\mathrm{d}t = \frac{k\Delta T}{\sqrt{\pi\kappa t_c}} = \frac{k\Delta T}{\delta_c}.$$

Howard (1964) proposed a simple model for convection at high *Ra*:

- Based on observations of boundary layers (BL) instabilities.
- Boundary layer grows by diffusion.
- BL becomes unstable when its Rayleigh number reaches a critical value.
- Cycle restarts.
- Ergodicity assumptions: horizontal average on an infinite layer equals time average on one cycle.
- Diffusive part of the cycle takes much longer than destabilisation part $\Rightarrow$ dominates the time average.

$$\Rightarrow \overline{T} = \frac{1}{t_c}\int_0^{t_c} \frac{\Delta T}{2}\,\mathrm{erf}\left(\frac{0.5 - z}{2\sqrt{\kappa t}}\right)\mathrm{d}t$$

  for the top boundary layer and something equivalent at the bottom.
- Heat flux

$$\overline{q} = \frac{1}{t_c}\int_0^{t_c} \frac{k\Delta T}{2\sqrt{\pi\kappa t}}\,\mathrm{d}t = \frac{k\Delta T}{\sqrt{\pi\kappa t_c}} = \frac{k\Delta T}{\delta_c}.$$

Howard (1964) proposed a simple model for convection at high *Ra*:

- Based on observations of boundary layers (BL) instabilities.
- Boundary layer grows by diffusion.
- BL becomes unstable when its Rayleigh number reaches a critical value.
- Cycle restarts.
- Ergodicity assumptions: horizontal average on an infinite layer equals time average on one cycle.
- Diffusive part of the cycle takes much longer than destabilisation part $\Rightarrow$ dominates the time average.

$$\Rightarrow \overline{T} = \frac{1}{t_c}\int_0^{t_c} \frac{\Delta T}{2}\,\mathrm{erf}\left(\frac{0.5-z}{2\sqrt{\kappa t}}\right)\mathrm{d}t$$

  for the top boundary layer and something equivalent at the bottom.
- Heat flux

$$\overline{q} = \frac{1}{t_c}\int_0^{t_c} \frac{k\Delta T}{2\sqrt{\pi\kappa t}}\,\mathrm{d}t = \frac{k\Delta T}{\sqrt{\pi\kappa t_c}} = \frac{k\Delta T}{\delta_c}.$$

Howard (1964) proposed a simple model for convection at high *Ra*:

- Based on observations of boundary layers (BL) instabilities.
- Boundary layer grows by diffusion.
- BL becomes unstable when its Rayleigh number reaches a critical value.
- Cycle restarts.
- Ergodicity assumptions: horizontal average on an infinite layer equals time average on one cycle.
- Diffusive part of the cycle takes much longer than destabilisation part $\Rightarrow$ dominates the time average.

  $$\Rightarrow \overline{T} = \frac{1}{t_c}\int_0^{t_c} \frac{\Delta T}{2}\,\mathrm{erf}\left(\frac{0.5 - z}{2\sqrt{\kappa t}}\right)\mathrm{d}t$$

  for the top boundary layer and something equivalent at the bottom.
- Heat flux

  $$\overline{q} = \frac{1}{t_c}\int_0^{t_c} \frac{k\Delta T}{2\sqrt{\pi\kappa t}}\,\mathrm{d}t = \frac{k\Delta T}{\sqrt{\pi\kappa t_c}} = \frac{k\Delta T}{\delta_c}.$$

Howard's model I

Howard (1964) proposed a simple model for convection at high *Ra*:

- Based on observations of boundary layers (BL) instabilities.
- Boundary layer grows by diffusion.
- BL becomes unstable when its Rayleigh number reaches a critical value.
- Cycle restarts.
- Ergodicity assumptions: horizontal average on an infinite layer equals time average on one cycle.
- Diffusive part of the cycle takes much longer than destabilisation part $\Rightarrow$ dominates the time average.
$$\Rightarrow \overline{T} = \frac{1}{t_c}\int_0^{t_c} \frac{\Delta T}{2}\,\mathrm{erf}\left(\frac{0.5 - z}{2\sqrt{\kappa t}}\right)\mathrm{d}t$$
for the top boundary layer and something equivalent at the bottom.
- Heat flux
$$\overline{q} = \frac{1}{t_c}\int_0^{t_c} \frac{k\Delta T}{2\sqrt{\pi\kappa t}}\,\mathrm{d}t = \frac{k\Delta T}{\sqrt{\pi\kappa t_c}} = \frac{k\Delta T}{\delta_c}.$$

- The thickness δ_c is determined by the instability of the boundary layer

$$\mathit{Ra}_\delta = \frac{g\alpha\Delta T\delta_c^3}{2\kappa\nu} = \frac{\mathit{Ra}}{2}\left(\frac{\delta_c}{d}\right)^3 = R_{\delta c}.$$

- Heat flux then scales as

$$\overline{q} = \frac{k\Delta T}{d}\left(\frac{\mathit{Ra}}{2R_{\delta c}}\right)^{1/3}.$$

- As noted by Howard (1964) $R_{\delta c}$ is different from the critical value for the stability of the whole layer since it concerns the destabilisation of a curved profile.
- This theory provides a scaling relation for the fluctuation time of the boundary layer:

$$t_c = \frac{\delta_c^2}{\pi\kappa} = \frac{d^2}{\pi\kappa}\left(\frac{2R_{\delta c}}{\mathit{Ra}}\right)^{2/3}.$$

Howard's model II

- The thickness δ_c is determined by the instability of the boundary layer

$$\mathit{Ra}_\delta = \frac{g\alpha\Delta T\delta_c^3}{2\kappa\nu} = \frac{\mathit{Ra}}{2}\left(\frac{\delta_c}{d}\right)^3 = R_{\delta c}.$$

- Heat flux then scales as

$$\overline{q} = \frac{k\Delta T}{d}\left(\frac{\mathit{Ra}}{2R_{\delta c}}\right)^{1/3}.$$

- As noted by Howard (1964) $R_{\delta c}$ is different from the critical value for the stability of the whole layer since it concerns the destabilisation of a curved profile.
- This theory provides a scaling relation for the fluctuation time of the boundary layer:

$$t_c = \frac{\delta_c^2}{\pi\kappa} = \frac{d^2}{\pi\kappa}\left(\frac{2R_{\delta c}}{\mathit{Ra}}\right)^{2/3}.$$

Howard's model II

- The thickness δ_c is determined by the instability of the boundary layer

$$\mathit{Ra}_\delta = \frac{g\alpha\Delta T\delta_c^3}{2\kappa\nu} = \frac{\mathit{Ra}}{2}\left(\frac{\delta_c}{d}\right)^3 = R_{\delta c}.$$

- Heat flux then scales as

$$\overline{q} = \frac{k\Delta T}{d}\left(\frac{\mathit{Ra}}{2R_{\delta c}}\right)^{1/3}.$$

- As noted by Howard (1964) $R_{\delta c}$ is different from the critical value for the stability of the whole layer since it concerns the destabilisation of a curved profile.
- This theory provides a scaling relation for the fluctuation time of the boundary layer:

$$t_c = \frac{\delta_c^2}{\pi\kappa} = \frac{d^2}{\pi\kappa}\left(\frac{2R_{\delta c}}{\mathit{Ra}}\right)^{2/3}.$$

Howard's model II

- The thickness δ_c is determined by the instability of the boundary layer

$$\mathit{Ra}_\delta = \frac{g\alpha\Delta T\delta_c^3}{2\kappa\nu} = \frac{\mathit{Ra}}{2}\left(\frac{\delta_c}{d}\right)^3 = R_{\delta c}.$$

- Heat flux then scales as

$$\overline{q} = \frac{k\Delta T}{d}\left(\frac{\mathit{Ra}}{2R_{\delta c}}\right)^{1/3}.$$

- As noted by Howard (1964) $R_{\delta c}$ is different from the critical value for the stability of the whole layer since it concerns the destabilisation of a curved profile.
- This theory provides a scaling relation for the fluctuation time of the boundary layer:

$$t_c = \frac{\delta_c^2}{\pi\kappa} = \frac{d^2}{\pi\kappa}\left(\frac{2R_{\delta c}}{\mathit{Ra}}\right)^{2/3}.$$

Experiments at very high *Ra*
Niemela et al. (2000)

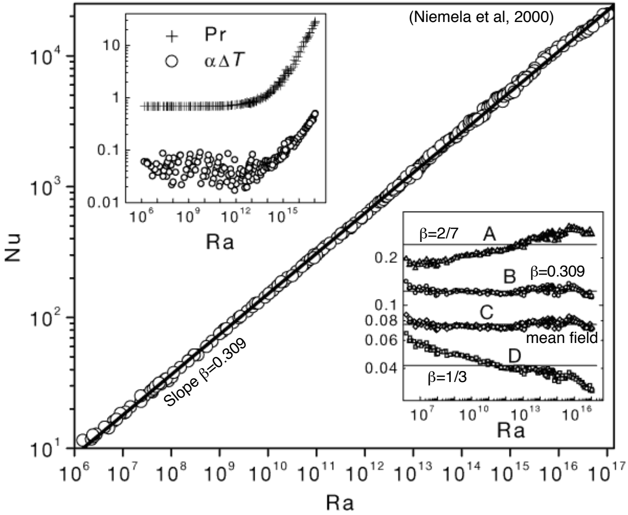

- Working fluid: cryogenic helium.
- *Pr* ~ 1
- 1 m–high tank.
- Exponent β close to but different from $1/3$.

- Bénard, H. (1900a). Les tourbillons celullaires dans une nappe liquide. Deuxième partie : procédés mécaniques et optiques d'examen. Lois numériques des phénomènes. **12**: 1309–1328.
- Bénard, H. (1900b). Les tourbillons celullaires dans une nappe liquide. Première partie : description générale des phénomènes. **12**: 1261–1271.
- Bénard, H. (1901). Les tourbillons celullaires dans une nappe liquide transportant la chaleur par convection en régime permanent. *Ann. Chim. Phys.* **23**: 62–144.
- Block, M. J. (1956). Surface Tension as the Cause of Bénard Cells and Surface Deformation in a Liquid Film. *Nature* **178**: 650–651.
- Boussinesq, J. (1903). *Théorie Analytique de la Chaleur*. Vol. 2. pp. 157–161. Gauthier-Villars.
- Busse, F. H. (1967). On the stability of two-dimensional convection in a layer heated from below. *J. Math. and Phys.* **46**: 140–149.
- Busse, F. H. and J. A. Whitehead (1971). Instabilities of convection rolls in a high Prandtl number fluid. *J. Fluid Mech.* **47**: 305–320.
- Grigné, C., S. Labrosse, and P. J. Tackley (2007a). Convection under a lid of finite conductivity in wide aspect ratio models: effect of continents on the wavelength of mantle flow. *J. Geophys. Res.* **112**: B08403.

- Grigné, C., S. Labrosse, and P. J. Tackley (2007b). Convection under a lid of finite conductivity: Heat flux scaling and application to continents. *J. Geophys. Res.* **112**: B08402.
- Guo, W., G. Labrosse, and R. Narayanan (2012). *The Application of the Chebyshev-Spectral Method in Transport Phenomena*. Berlin: Springer-Verlag.
- Howard, L. N. (1964). "Convection at High Rayleigh number". *Proceedings of the Eleventh International Congress of Applied Mechanics*. Ed. by H. Gortler. New York: Springer-Verlag, 1109–1115.
- Krishnamurti, R. (1973). Some further studies on the transition to turbulent convection. *J. Fluid Mech.* **60**: 285–303.
- Labrosse, S., A. Morison, R. Deguen, and T. Alboussière (2018). Rayleigh-Bénard convection in a creeping solid with a phase change at either or both horizontal boundaries. *J. Fluid Mech.* **846**: 5–36.
- Malkus, W. and G. Veronis (1958). Finite amplitude cellular convection. *J. Fluid Mech.* **4**: 225–260.
- Manneville, P. (2004). *Instabilities, Chaos and Turbulence - An introduction to nonlinear dynamics and complex systems*. London: Imperial College Press.
- Niemela, J. J., L. Skrbek, K. R. Sreenivasan, and R. J. Donnelly (2000). Turbulent convection at very high Rayleigh numbers. *Nature* **404**: 837–841.

- Oberbeck, A. (1879). Über die Wärmeleitung des Flüssigkeiten bei Berücksichtigung des Strömungen infolge von Temperaturdifferenzen. *Ann. Phys. Chem.* **7**: 271–292.
- Pearson (1958). On convection cells induced by surface tension. *J. Fluid Mech.* **4**: 489–500.
- Pouilloux, L., E. Kaminski, and S. Labrosse (2007). Anisotropic rheology of a cubic medium and implications for geological materials. *Geophysical Journal International* **170**: 876–885.
- Rayleigh, L. (1916). On convection currents in a horizontal layer of fluid, when the higher temperature is on the under side. *Phil. Mag.* **32**: 529–546.
- Ricard, Y., S. Labrosse, and F. Dubuffet (2014). Lifting the cover of the cauldron: Convection in hot planets. *Geochem. Geophys. Geosyst.* **15**: 4617–4630.
- Schlüter, A., D. Lortz, and F. Busse (1965). On the Stability of Steady Finite Amplitude Convection. *J. Fluid Mech.* **23**: 129–144.
- Sotin, C. and S. Labrosse (1999). Three-dimensional Thermal convection of an isoviscous, infinite–Prandtl–number fluid heated from within and from below: applications to heat transfer in planetary mantles. *Phys. Earth Planet. Inter.* **112**: 171–190.